Downloaded from rsta.royalsocietypublishing.org

PHILOSOPHICAL TRANSACTIONS OF THE ROYAL SOCIETY A MATHEMATICAL, PHYSICAL & ENGINEERING SCIENCES

The Solid State Dehydration of d Lithium Potassium Tartrate Monohydrate is Completed in Two Rate Processes II. The Nucleation and Growth Second Reaction and Dehydration Mechanism

Andrew K. Galwey, Genevieve M. Laverty, Nickolai A. Baranov and Vladimir B. Okhotnikov

Phil. Trans. R. Soc. Lond. A 1994 **347**, 157-184
doi: 10.1098/rsta.1994.0043

Email alerting service

Receive free email alerts when new articles cite this article - sign up in the box at the top right-hand corner of the article or click **here**

To subscribe to *Phil. Trans. R. Soc. Lond. A* go to:
http://rsta.royalsocietypublishing.org/subscriptions

This journal is © 1994 The Royal Society

Downloaded from rsta.royalsocietypublishing.org

The solid state dehydration of *d* lithium potassium tartrate monohydrate is completed in two rate processes

II. The nucleation and growth second reaction and dehydration mechanism

By Andrew K. Galwey[1], Geneviève M. Laverty[1], Nickolai A. Baranov[2] and Vladimir B. Okhotnikov[2]

[1] *School of Chemistry, The Queen's University of Belfast, Belfast BT9 5AG, U.K.*
[2] *Institute of Solid State Chemistry, Derzhavina 18, Novosibirsk 630091, Russia*

A kinetic and mechanistic study has been undertaken of the nucleation and growth reaction that is the second of the two consecutive rate processes that occur during the dehydration of *d* lithium potassium tartrate monohydrate. Electron microscopic examinations of the cleaved surfaces of partly reacted crystals show the development of three-dimensional nuclei that are composed of small crystals of the anhydrous product and above 450 K there is evidence of intranuclear melting. Consistent with this model, the second reaction obeys the Avrami–Erofe'ev equation $\{[-\ln(1-\alpha)]^{\frac{1}{2}} = kt\}$. Overall rates of the dehydrations of single crystals and of crushed powder samples were closely similar. The activation energy for dehydration was 150–160 kJ mol^{-1} for both first (reported in part I, preceding paper) and second reactions and for both single crystal and crushed powder reactants. The addition of product crystallites to the reactant reduced sharply, or eliminated, the induction period to the nucleation and growth process.

From consideration of the kinetic characteristics, together with the textural changes observed microscopically, we conclude that the following mechanism very satisfactorily accounts for our results. The first reaction proceeds to the dehydration of all crystal surfaces, representing water losses from a layer *ca.* 10 μm thickness. This deceleratory process occurs initially in a structure resembling that of the reactant but later the increasing water site vacancy concentration results in increasing reactant disorder and possibly includes fusion of the outer layer. When the first reaction water evolution has slowed, recrystallization to the structure of the anhydrous product occurs at a limited number of sites to generate germ nuclei that effectively act as seed crystals for nucleus growth. During the second reaction the reactant–product contact interface is identified as a zone of diffusive water loss, similar to that described for the first reaction. Here, however, the product crystallites promote reorganization of dehydrated material, thereby opening channels for water escape and continually exposing new hydrate surfaces at which dehydration continues. This product recrystallization enables advance of the nucleus interface to be maintained, so that rates of both first and second reactions are subject to control by diffusive loss of water from an active boundary of the reactant. Product reorganization removes the inhibiting character of accumulated product layer by introducing escape channels for water loss so that interface advance continues and, although spasmodic, this migrates forward at a constant average linear rate.

Phil. Trans. R. Soc. Lond. A (1994) **347**, 157–184
Printed in Great Britain

© 1994 The Royal Society

The Royal Society is collaborating with JSTOR to digitize, preserve, and extend access to *Philosophical Transactions: Physical Sciences and Engineering.*
www.jstor.org

Downloaded from rsta.royalsocietypublishing.org

The work is of interest because kinetic measurements have been obtained for both of the consecutive rate processes that contribute to the overall reaction. The controls of both are shown to be closely similar. The reaction model proposed here provides insight into the structure of the dehydration interface and the mechanism of water release.

1. Introduction

The dehydration of *d* lithium potassium tartrate monohydrate merits investigation because reliable kinetic data can be measured for the two distinct and different consecutive rate processes that yield the anhydrous crystalline product salt. The first reaction is deceleratory and has been shown in part I (preceding paper) to be controlled by the rate of diffusive water loss through a developing array of vacant H_2O-accommodating sites within a thin surface zone of reactant crystallites. This paper is concerned with the second reaction, which is a nucleation and growth process (Brown *et al.* 1980). Compact nuclei, composed of the recrystallized product, the anhydrous salt, grow because of advance of an active dehydration interface into the unchanged reactant monohydrate. We are aware of no other reactant for which detailed rate studies of two consecutive and kinetically distinct dehydration processes are practicable. These investigations have, therefore, been undertaken to continue the well-established tradition of using observations on dehydrations to extend knowledge of the mechanisms of solid state reactions (Garner 1955; Niepce & Watelle-Marion 1973; Brown *et al.* 1980; Galwey & Laverty 1990*a*). Dehydrations are often regarded as relatively simple chemical reactions. The relative thermal stability of the reactant was an important consideration in identifying this salt as being of interest for study. It is experimentally helpful that large, relatively perfect crystals are easily grown.

It has been found difficult to provide a useful classification of the many solid state dehydrations that have been investigated (Galwey 1985, 1990, 1992). One possible criterion is to distinguish (Galwey & Laverty 1990*a*) the following two types. (i) Deceleratory reactions in which water evolution is controlled by diffusive escape from within a largely unreorganized structure that does not recrystallize during dehydration (external interface). (ii) Nucleation and growth processes where reaction occurs at an advancing active zone within which there is reactant to product recrystallization (internal interface). The reaction described in part I is of the first of these types (i) and is followed by the nucleation and growth second stage of type (ii) that is reported here. We focus particular attention on the mechanism of the interface processes and the relation between both reactions for which we have obtained kinetic data.

Some progress has been made in elucidating the form and function of reaction interfaces in nucleation (Galwey & Laverty 1990*b*) and growth (Galwey 1985, 1990, 1992) processes. For several solid-state reactions these zones have been shown to be more complicated than an advancing thin layer, perhaps of single ionic thickness, within which there was concurrent water elimination and phase transformation. This simple model appears to be implicitly assumed in the earlier theoretical analyses (Garner 1955). More recent studies, however, such as those by Boldyrev *et al.* (1987) have discussed progressive changes of the reactant crystal structure in advance of the approaching reaction interface. The thickness of the reaction zone in $Li_2SO_4 . H_2O$

Downloaded from rsta.royalsocietypublishing.org

dehydration is reported to be about 150 μm. Galwey *et al.* (1990) used electron microscopy to detect textural changes in the vicinity of the dehydration interface for the same reaction. It is concluded that the reaction zone is composed of a layer of hydrate from which water is progressively lost as the recrystallization boundary approaches, bringing with it the channels that enable intranuclear released water vapour to escape.

Galwey *et al.* (1981) concluded that, in vacuum, alums initially lost water from all crystal faces but the extent of such water loss was small. At suitable surface sites, probably zones of distortion and including dislocations, growth nuclei were formed. Nuclei were identified as structures specifically capable of temporarily retaining a proportion of the product water and it is concluded (Galwey & Guarini 1993) that this water is essential for promotion of the difficult recrystallization step (hydrated alum transformation to the recrystallized lower hydrate(s)). Dehydration is, therefore, regarded as an autocatalytic process involving the adsorbed volatile product. Other work (Galwey & Mohamed 1987) demonstrated, for these alums, that strain did not result in crack propagation in advance of the interface. Intranuclear cracks, permeating the product assemblage, result from shrinkage and afford escape channels for the water released. The ability of water to promote recrystallization is inherently less probable in this salt's dehydration, which has been studied in a higher temperature range (more than about 410 K) than that investigated for alums (less than about 320 K).

d Lithium potassium tartrate monohydrate was selected to enable comparative studies to be made for the two rate processes that contribute (consecutively) to the completed dehydration and the relations between them are discussed. We are aware of no previous investigation of the dehydration of lithium potassium tartrate hydrates, other than those that constitute our own extended work. We have shown (Baranov *et al.* 1990) that the reactivities of the compositionally identical lithium potassium tartrate hydrates vary with anion stereochemistry. Salts containing the same cations, lithium and potassium, with the *dl* (Bhattamisra *et al.* 1992) and *meso* (Galwey *et al.* 1992) forms of the anion comprehensively melt during dehydration. This contrasts with the behaviour reported here for the salt containing the *d* form of the anion, where a vitreous, perhaps molten, superficial layer is formed during the first rate process and the second is identified as proceeding in a solid reactant. These marked differences in kinetic characteristics are explained by the hydrophilic character of the anion which can be expected to retain water and to form intermediate glassy structures through local modifications of the extensive hydrogen bonding.

2. Experimental

Throughout this paper the kinetic data and the microscopic observations were obtained using the same reactant preparation (salt B) and apparatus as described in part I. Whenever possible, experimental measurements extended across both first and second reactions to enable comparisons of kinetic data to be based on the completed dehydrations of the individual samples investigated.

Reactant. The preparation and composition of salt B, *d* $LiKC_4H_4O_6.H_2O$, have already been reported in part I. Limited series of experiments using other similarly prepared reactant samples confirmed the reproducibility of kinetic behaviour for different batches of salt.

Apparatus. Dehydration rates were obtained from measurements, at appropriate

PHILOSOPHICAL TRANSACTIONS OF THE ROYAL SOCIETY A MATHEMATICAL, PHYSICAL & ENGINEERING SCIENCES
PHILOSOPHICAL TRANSACTIONS OF THE ROYAL SOCIETY A MATHEMATICAL, PHYSICAL & ENGINEERING SCIENCES

Downloaded from rsta.royalsocietypublishing.org

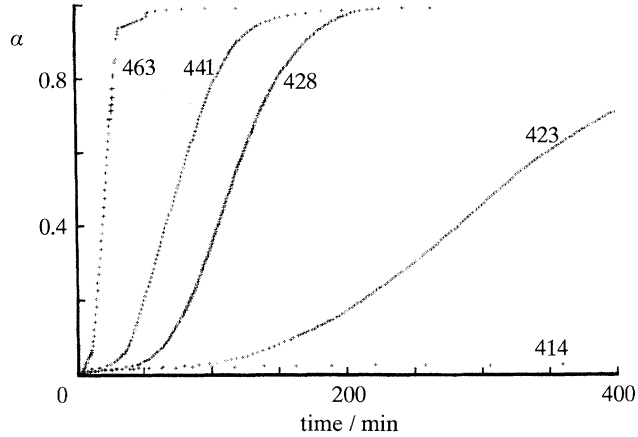

Figure 1. Representative fractional reaction α–time plots for the isothermal dehydrations of *d* lithium potassium tartrate monohydrate single crystals. The contribution from the first deceleratory reaction is small (*ca.* 4%) and the sigmoidal nucleation and growth process is dominant. Values in Kelvins.

time intervals, of the pressure of water vapour evolved in a pre-evacuated glass apparatus using a Baratron diaphragm gauge while the reactant salt was maintained at the constant reaction temperature. Pressure of water vapour, time and temperature were recorded automatically at pre-specified time intervals for subsequent kinetic analyses. The experimental method has been described in detail in Carr & Galwey (1986).

Electron Microscopy. Salt samples, reacted to various known extents, were examined in a Jeol 35CF scanning electron microscope (SEM). Observations included both external crystal faces and internal textural structures revealed by cleavage after reaction. Features were accepted as characteristic only when these were reproducible and seen on more than one prepared specimen. Some optical microscopy was also undertaken.

3. Results and discussion

Representative fractional reaction α–time plots for isothermal dehydrations of *d*-$LiKC_4H_4O_6.H_2O$ in the pre-evacuated apparatus at comparable temperatures, across the range of these investigations, are shown for single crystal and crushed crystal reactants in figures 1 and 2 respectively. For single crystals the first reaction is completed at $\alpha \approx 0.04$ (figure 1) and the subsequent sigmoidal water-evolution–time curve for the second reaction is the dominant process. The first reaction is much more extended during dehydration of the powder (figure 2) and the onset of the subsequent (second) sigmoidal water-evolution–time process occurs somewhat less rapidly.

Systematic kinetic investigations have been completed for the dehydrations of both single crystal and crushed crystal samples in which interpretation of the kinetic data included consideration of microscopic observations of the textural changes that accompanied water removal. Following previous practice (Galwey & Pöppl 1984), we find it convenient to report and discuss the microscopic observations first, thus enabling the interpretation of the kinetic data to be based on a knowledge of the systematic changes in texture that occur as reaction progresses (Oswald 1980).

Downloaded from rsta.royalsocietypublishing.org

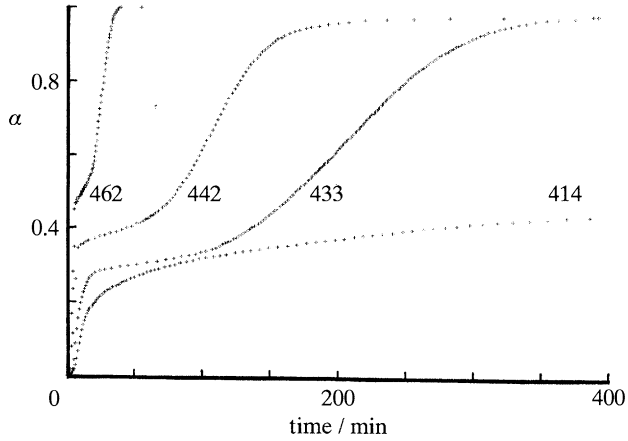

Figure 2. Representative α–time plots for the isothermal dehydration of *d* lithium potassium tartrate monohydrate crushed powder. The contribution from the first reaction (*ca.* 30–40%) is much greater than that for single crystals (compare with Figure 1).

It has already been shown (part I) that the first reaction results in water losses from crystal faces through the development of a concentration gradient at water-accommodating sites within a superficial disordered vacancy structure. Initiation of the second reaction must, therefore, take place in, at or on crystals that have already undergone substantial superficial modification, probably extending to local melt or vitreous phase formation.

(*a*) *Stoichiometry*

The composition of the reactant (C, 22.40 ± 0.20%; H, 2.85 ± 0.05%) corresponded closely with theoretical expectation for the monohydrate (C, 22.65%; H, 2.85%). Mass losses on completion of dehydration for single crystals (9.3 ± 0.8%) were somewhat greater than expectation for the monohydrate (8.5%) whereas losses for crushed crystals were closer at 8.7 ± 0.7%. Water yields determined from evolved pressures in the calibrated-volume apparatus (expressed as mass losses) corresponded to 8.9 ± 0.8% for single crystals and 8.6 ± 0.7% for crushed crystals. Volatile product condensation with cold traps at 77 K and 213 K, measured for dehydrations completed throughout the temperature range of the studies, showed no perceptible yields of other possible gaseous products, e.g. CO and CO_2. Although the prepared salt B may retain small quantities of included or surface adsorbed water, the reaction may be expressed as the evolution of one molecule of water of crystallization without perceptible anion breakdown (see Galwey & Laverty 1993)

$$d\text{-}LiKC_4H_4O_6 . H_2O \rightarrow d\text{-}LiKC_4H_4O_6 + H_2O.$$

(*b*) *Scanning electron microscopy*

There was no evidence of comprehensive melting of the reactant within the temperature interval investigated during the present kinetic studies, 379–475 K. Evidence of possible vitreous phase formation was limited to the superficial layer, as discussed in part I. The residual anhydrous product consisted of coherent aggregates of small crystallites; such coherent assemblages were pseudomorphic with the original reactant single crystals. During dehydrations of crushed crystals, however, there was sintering of the individual particles to form a coherent, fairly hard and rigid concretion that was the residual product.

PHILOSOPHICAL TRANSACTIONS OF THE ROYAL SOCIETY A MATHEMATICAL, PHYSICAL & ENGINEERING SCIENCES
PHILOSOPHICAL TRANSACTIONS OF THE ROYAL SOCIETY A MATHEMATICAL, PHYSICAL & ENGINEERING SCIENCES

Downloaded from rsta.royalsocietypublishing.org

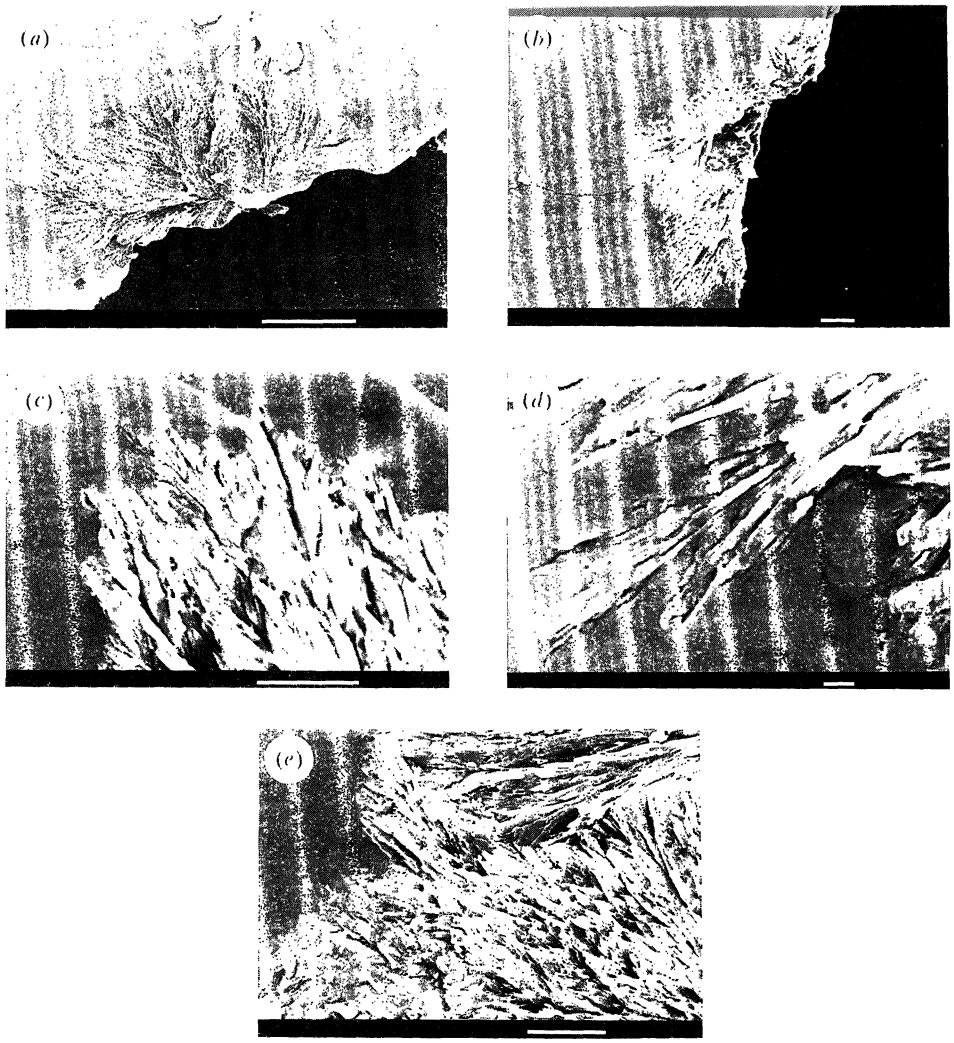

Figure 3. Partly dehydrated single crystal of *d*-$LiKC_4H_4O_6.H_2O$ ($\alpha = 0.12$ at 434 K) cleaved after reaction to show textured nuclei in section together with the relatively smooth unreacted material. Intranuclear crystallites are of length *ca.* 10 μm, thickness *ca.* 1 μm, and show alignment. (Scale bars: (*a*) 100 μm; (*b*), (*c*), (*e*) 10 μm; (*d*) 1.0 μm.)

Conditions within the SEM were sufficiently severe to cause limited surface retexturing during observations and this restricted our ability to examine the unreacted monohydrate. There was an effective ceiling on magnification of about $\times 5000$. At magnifications of $\times 3000$ and above there was a slow deterioration of surfaces, particularly those which included cleaved faces of unreacted material. This could be seen as a progressive rounding of sharp edge features together with the appearance and development of irregular crack systems. The photographs used to illustrate textural features of interest here have been selected to minimize the artefacts arising as a consequence of beam damage.

PHILOSOPHICAL TRANSACTIONS OF THE ROYAL SOCIETY A MATHEMATICAL, PHYSICAL & ENGINEERING SCIENCES
PHILOSOPHICAL TRANSACTIONS OF THE ROYAL SOCIETY A MATHEMATICAL, PHYSICAL & ENGINEERING SCIENCES

Downloaded from rsta.royalsocietypublishing.org

Figure 4

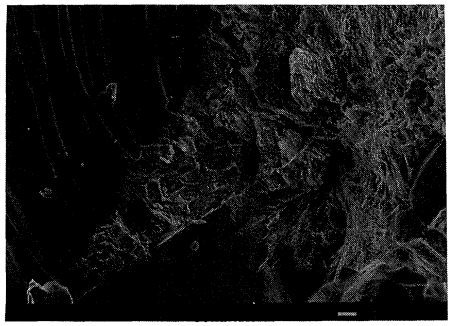

Figure 5

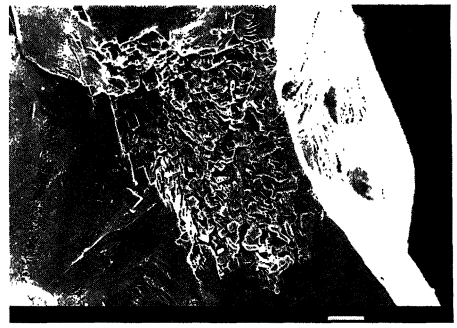

Figure 4. Section of a partly dehydrated single crystal of *d*-$LiKC_4H_4O_6.H_2O$ ($\alpha = 0.20$ at 423 K), showing extended nucleus growth along one side of a crack present before reaction. (Scale bar 10 μm.)

Figure 5. Section of a partly dehydrated single crystal of *d*-$LiKC_4H_4O_6.H_2O$ ($\alpha = 0.14$ at 420 K). The nucleus is located beneath a texturally modified crystal face. (Scale bar 10 μm.)

The nucleation and growth reaction in single crystals

410–435 K. Optical microscopic examinations of partially dehydrated salt ($\alpha \approx 0.2$) revealed the presence of approximately hemispherical white zones, identified as nuclei, that were generated at, or very near, the surfaces and frequently at the corners of the transparent crystals. The sizes of these zones increased with the extent of reaction (fractional reaction, α) but varied appreciably within any partially reacted crystal, suggesting non-instantaneous nucleation (Brown *et al.* 1980).

Nuclei were readily recognized during SEM examinations of cleaved faces of crystals, sectioned after partial dehydration. The recrystallized zones markedly contrast with the flat fracture surfaces of the unreacted salt, typical textures are shown in figure 3*a*, *b* ($\alpha = 0.12$ at 434 K). The anhydrous intranuclear material is composed of slab-like crystallites, the sizes of which were difficult to measure, but typical values were estimated to be: slab edge *ca.* 10 μm; thickness *ca.* 1 μm; and these particles were separated by open channels of 0.1–0.2 μm. Slabs are aligned, maintain edge contact and generally radiate outwards from the original nucleation sites between which the channels provide escape routes for the water evolved. The irregular reaction interface at the periphery of the advancing nucleus is shown in figure 3*c*, *d* ($\alpha = 0.12$ at 434 K, the photograph at the higher magnification shows evidence of the onset of SEM beam damage). Slab orientations are incoherent and misaligned at regions of nucleus overlap, figure 3*e* ($\alpha = 0.12$ at 434 K).

Figure 4 ($\alpha = 0.20$ at 423 K) provides evidence that there were different rates of nucleus expansion on either side of a crack, probably present in the crystal before reaction but penetrating a region of crystal that was previously effectively homogeneous. Dehydration has advanced preferentially on one side of this water escape channel but crystallization on the other side has not similarly developed. Product phase recrystallization evidently can proceed once crystalline product is present and an interface has been established but may not occur on the other side of the water escape channel if contact with the product structure is less effective. Nuclei are often only approximately hemispherical, with irregular, serrated slab development penetrating adjoining reactant at each periphery.

The sectioned nucleus in figure 5 ($\alpha = 0.14$ at 420 K) is located beneath a

PHILOSOPHICAL TRANSACTIONS OF THE ROYAL SOCIETY A MATHEMATICAL, PHYSICAL & ENGINEERING SCIENCES

PHILOSOPHICAL TRANSACTIONS OF THE ROYAL SOCIETY A MATHEMATICAL, PHYSICAL & ENGINEERING SCIENCES

Downloaded from rsta.royalsocietypublishing.org

Figure 6

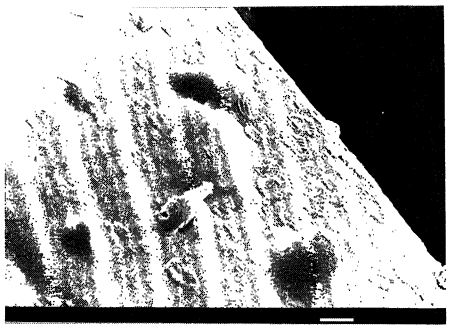

Figure 7

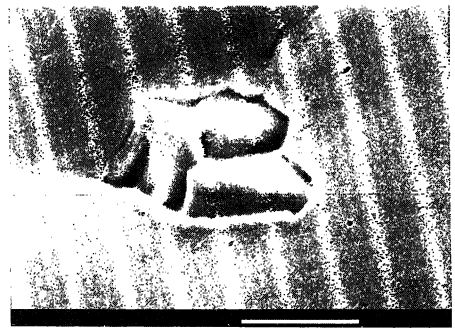

Figure 6. Surface of a partly dehydrated single crystal of *d*-$LiKC_4H_4O_6.H_2O$ ($\alpha = 0.14$ at 420 K). Blister-like modifications are identified as accumulations of water vapour before its release. (Scale bar 10 μm.)

Figure 7. Surface of a partly dehydrated single crystal of *d*-$LiKC_4H_4O_6.H_2O$ ($\alpha = 0.42$ at 425 K). A rare occurrence of surface penetration by crystalline material. (Scale bar 10 μm).

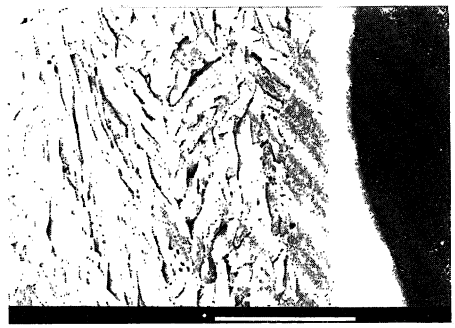

Figure 8. Section of a reacted zone in a partly dehydrated single crystal of *d*-$LiKC_4H_4O_6.H_2O$ ($\alpha = 0.15$ at 433 K). The outer coherent layer identified with the first reaction has a different texture from the small intranuclear product crystallites generated beneath. (Scale bar 10 μm.)

texturally modified crystal face (see also figure 6*c*, *d* in part I). Surface modifications observed during the second reaction include blister-like protuberances, as in figure 6 ($\alpha = 0.14$ at 420 K), attributable to steam accumulations prior to release; the surface scarring is identified as sites of burst bubbles from previous water emissions. Occasionally the surface layer was penetrated by crystalline material, figure 7 ($\alpha = 0.42$ at 425 K). More usually, however, the texture of the superficial coherent layer, identified with the first reaction, did not undergo obvious recrystallization but in section was readily distinguished from the intranuclear product generated immediately beneath it, figure 8 ($\alpha = 0.15$ at 433 K).

460–475 K. Textural changes occurring during salt dehydration in this higher temperature interval were different from those described above. Representative features, regarded as significant, as illustrated in figure 9*a–e*, observed for a single crystal after partial reaction ($\alpha = 0.40$ at 460 K) and subsequent cleavage. The product nuclei contained parallel pores or channels (sometimes 10×100 μm); these were often parallel and always showed rounded peripheries.

Cleavage of crystals, partly dehydrated above 460 K, exposed planar faces across the unreacted salt, but such cleavage cracks did not propagate across product

Downloaded from rsta.royalsocietypublishing.org

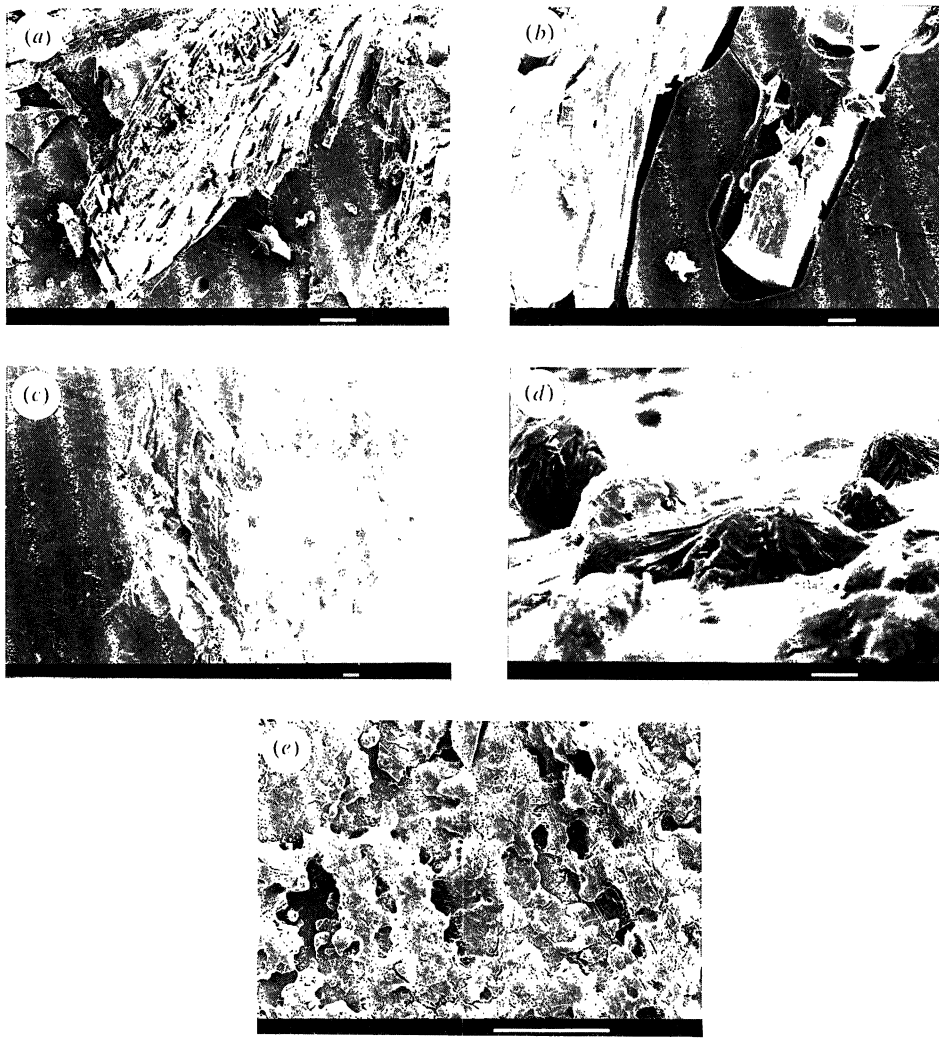

Figure 9. Sections (*a*), (*b*), (*c*) and surfaces (*d*), (*e*) of a partly dehydrated single crystal of *d*-$LiKC_4H_4O_6.H_2O$ ($\alpha = 0.40$ at 460 K). At this higher reaction temperature contact between product and reactant at nucleus peripheries is reduced by the generation of channels. Outer surfaces are distorted and show evidence of local liquefaction together with bubbles that are associated with release of product water vapour from nuclei beneath. (Scale bars: (*a*), (*e*) 100 μm; (*b*), (*c*), (*d*) 10 μm.)

assemblages, so that nuclei were not sectioned by the same fracture plane, figure 9*a* ($\alpha = 0.40$ at 460 K). This is ascribed to the loss of reactant-product contact within the reaction zone: gaps that had developed around the nucleus during growth are evident in figure 9*b* (which shows, at higher magnification, an area from the top right hand corner of figure 9*a*). A different sectioned nucleus is shown in figure 9*c*, in which it can be seen that the reactant surface above the nucleus is distorted by protuberances and bubbles, shown in greater detail in figure 9*d*. These bubbles are identified as distortion of a vitreous surface during escape of steam from subsurface dehydration. An area of extensively distorted surface, which appears to have

Downloaded from rsta.royalsocietypublishing.org

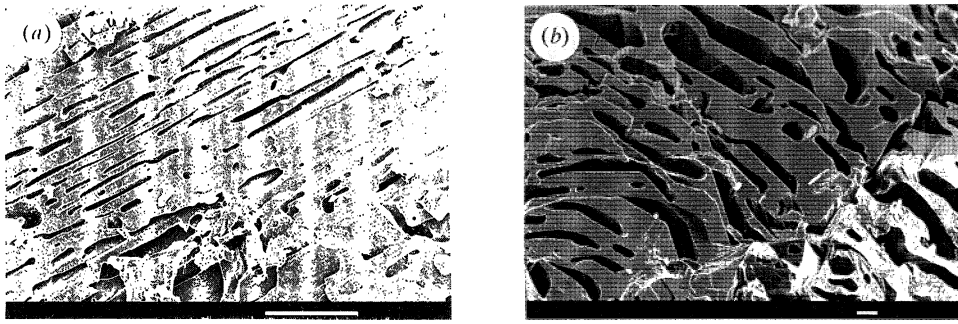

Figure 10. Cleaved single crystal of d-$LiKC_4H_4O_6.H_2O$, after complete dehydration ($\alpha = 1.00$ at 463 K). Pores in the product are rounded, elongated and show some parallelism. (Scale bars: (a) 100 μm; (b) 10 μm.)

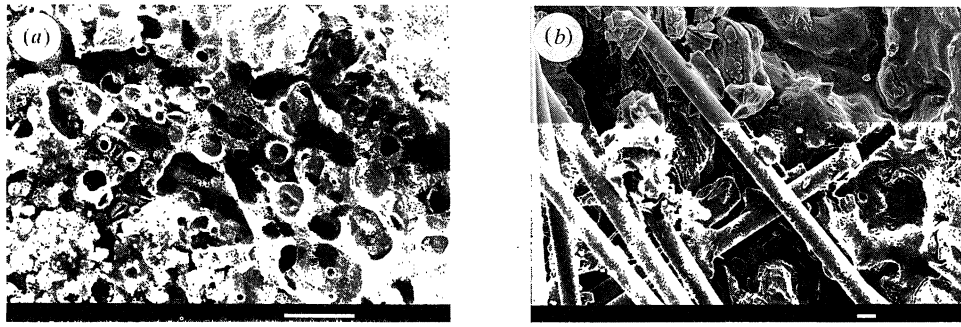

Figure 11. Surfaces of a single crystal of d-$LiKC_4H_4O_6.H_2O$ after complete dehydration ($\alpha = 1.00$ at 455 K). Crystal features are absent, and the burst bubbles and penetration by glass fibres are evidence of superficial liquefaction. (Scale bars both 10 μm.)

undergone local liquefaction, again with the development of rounded features, evidence of surface tension control, is shown in figure 9e.

The internal textures of dehydrated ($\alpha = 1.00$ at 463 K) crystals, subsequently cleaved, are shown in figure 10a, b. As in the nuclei seen in figure 9, there is the parallel disposition of elongated holes with rounded boundaries. The textures of outer surfaces of dehydrated crystals ($\alpha = 1.00$ at 455 K) are shown in figure 11a, where the rounded craters are identified as burst bubbles at an almost liquid surface, and in figure 11b, where glass fibres, used to retain the crystal in the reaction vessel, have become embedded in the semi-liquid boundary layer. This is strong evidence of superficial liquefaction, fusion or vitreous phase formation. The rounded features are characteristic of control by surface tension forces and there is an absence of the flat faces and sharp edges that are a feature of crystallinity.

Comment. The pattern that emerges from these microscopic examinations, exemplified by figures 9–11, is that there are textural modifications during dehydration due to superficial fusion of the crystals that does not, however, proceed to comprehensive liquefaction. The residual solid particles are pseudomorphic with the reactant crystals. Evidently bubbles (Guarini & Rustici 1987) are generated within the liquefied outer layer and provide the escape mechanism for water released within the developing nuclei beneath. There is a possibility that a proportion of such water may be temporarily accommodated within the structure of the outer disorganized region of the solid and is retained there through hydrogen bonding in

Downloaded from rsta.royalsocietypublishing.org

the vitreous phase. The consequent local reduction in viscosity permits bubble formation, followed by collapse after escape of the steam, and subsequent healing of the surface, rather than the cracking that would be expected for crystalline material (figures 9*c*, *d* and 11*a*).

The textural evidence from figure 9*a*, *b* is that water is released from an interface at which appreciable gaps develop around the nucleus periphery. Nucleus growth (at more than 460 K) occurs through the generation of individual slabs and the gaps between these, arising from the shrinkage after water loss, are the channels that give the solid product its characteristic open structure and provide paths for escape of water (figure 10). The rounded peripheries of these structures indicate mobility of the surface species involved. The absence of comprehensive and coherent reactant–product contact at the interface is consistent with diffusive water loss from adjoining regions of the crystal into the intranuclear pore spaces. Subsequent structural reorganization of the dehydrated boundary of the reactant develops from contacts with anhydrous crystalline product, acting as seed crystals. The occurrence of a nucleation and growth reaction is, in itself, evidence that the generation of a product phase crystallite is an unusual, rare or energetically difficult event. The fluid characteristics of the surface, including bubble-like structures and closing of pores, suggest that this layer does not reorganize to form a crystalline product until the bulk of the locally available water has been eliminated. We conclude, therefore, that two distinct steps contribute to nucleus growth, dehydration followed by recrystallization with detachment so that the dehydration of a new layer of reactant becomes possible. Nucleus growth is seen as a stepwise process and, if the rates of the two contributory steps are different, advance is spasmodic.

Although it is usually accepted (Brown *et al.* 1980) that nucleation is a surface phenomenon, our evidence shows that, here, nucleation and growth commences after the generation of a coherent, comprehensive layer of dehydrated material across all surfaces. The superficial viscous material is the dehydrated product of the first reaction and its texture is recognizably distinct from that characteristic of the nuclei developed beneath.

Crystal reacted with dehydrated salt

The dehydrated crystal in figure 12 ($\alpha = 1.00$ at 425 K) was, before reaction, entirely surrounded by crushed powder of a previously dehydrated crystal. The residual product is pseudomorphic with the reactant and no significant quantity of the anhydrous powder has adhered to it.

Reaction in initial additional water vapour.

The presence of water vapour in the reaction vessel before dehydration resulted in the textural changes illustrated in figure 13*a*, *b* ($\alpha = 1.00$ at 423 K). The original external crystal faces were relatively smoother (figure 13*a*), appreciably more sintered and less porous, than surfaces correspondingly reacted in lower water vapour pressures (*cf.* part I, fig. 6*a*). Again there is evidence that increased availability of water vapour enhances surface mobility. A new feature, not found under other reaction conditions, was the development of relatively large pores, up to *ca.* 25 μm diameter, within the crystal bulk, seen in section in the cleavage surface (figure 13*b*). This is apparently a further consequence of the increased reactant plasticity in water vapour.

PHILOSOPHICAL TRANSACTIONS OF THE ROYAL SOCIETY A MATHEMATICAL, PHYSICAL & ENGINEERING SCIENCES
PHILOSOPHICAL TRANSACTIONS OF THE ROYAL SOCIETY A MATHEMATICAL, PHYSICAL & ENGINEERING SCIENCES

Downloaded from rsta.royalsocietypublishing.org

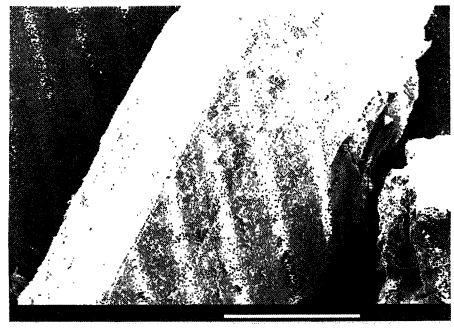

Figure 12. Crystal of *d*-$LiKC_4H_4O_6.H_2O$ after complete dehydration ($\alpha = 1.00$ at 425 K) initially surrounded loosely by crushed, dehydrated product. The anhydrous powder did not significantly adhere to the reactant crystal. (Scale bar 1 mm.)

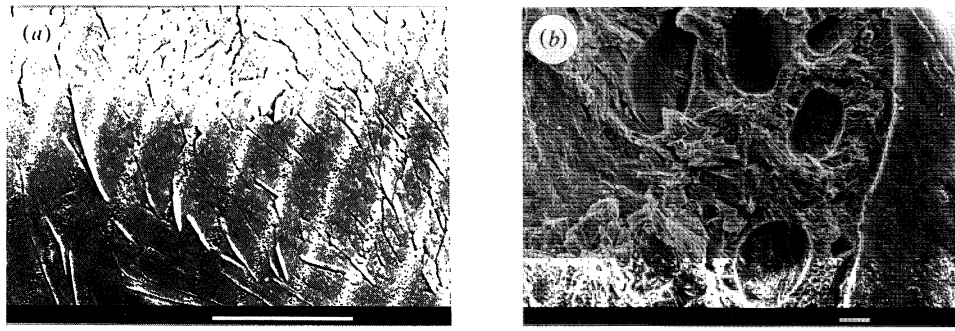

Figure 13. Surface (*a*) and section (*b*) of a crystal of *d*-$LiKC_4H_4O_6.H_2O$, dehydrated ($\alpha = 1.00$) at 423 K, in the presence of water vapour admitted before reaction. External crystal faces are smoother and large pores develop in the crystal bulk. (Scale bars both 10 μm.)

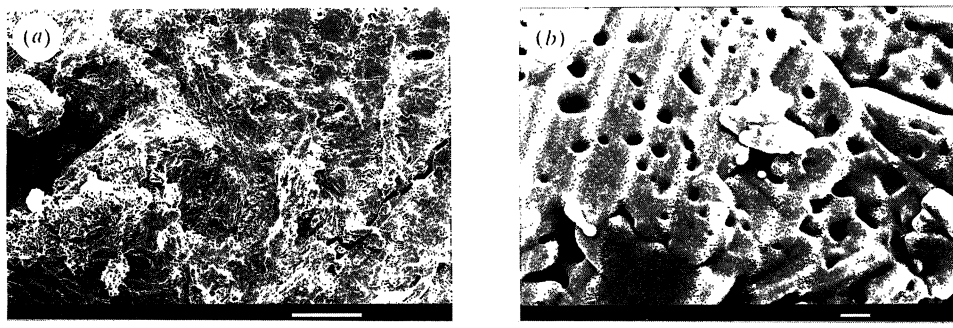

Figure 14. Surface of a crystal of *d*-$LiKC_4H_4O_6.H_2O$ after two successive dehydrations ($\alpha = 1.00$ at 461 K and 423 K) with intermediate rehydration at 290 K. Features are smooth and rounded, indicating a superficial boundary layer controlled by surface tension forces. (Scale bars (*a*) 100 μm; (*b*) 1.0 μm.)

Multiple dehydrations

The surfaces of a crystal after two successive dehydrations ($\alpha = 1.00$ at 461 and 423 K respectively, with intermediate rehydration at *ca.* 290 K) are shown in figure 14*a*, *b*. Rounded textural features are again apparent and the crystal face is penetrated by numerous small pores, often less than 1 μm in diameter. The smooth

Downloaded from rsta.royalsocietypublishing.org

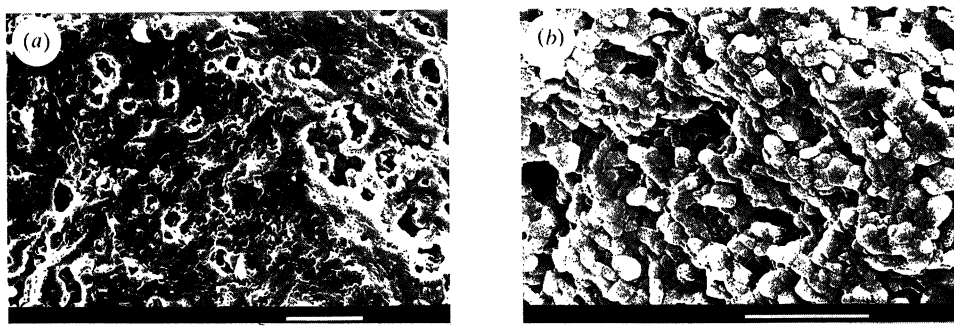

Figure 15. Surface and internal textures of a crystal ($\alpha = 1.00$) of d-$LiKC_4H_4O_6.H_2O$ after seven successive dehydration/rehydration cycles (at 423 K and 290 K respectively). The surface (a) is approximately planar but porous, while the internal texture (b) is composed of small crystallites. (Scale bars both 10 μm.)

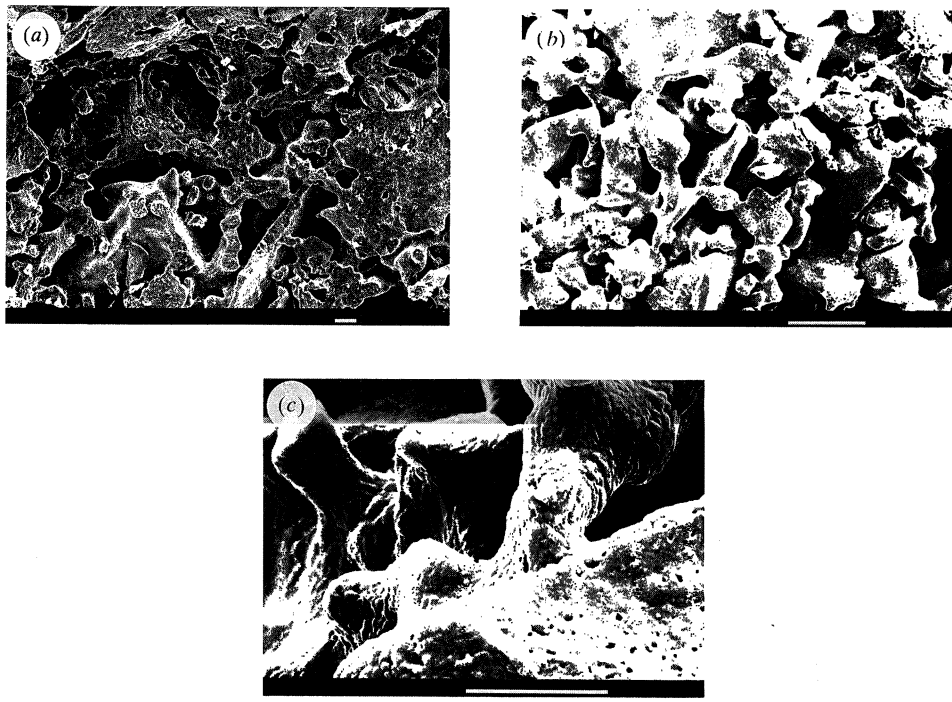

Figure 16. (a), (c) Crushed d-$LiKC_4H_4O_6.H_2O$ after dehydration ($\alpha = 1.0$ at 423 K) commencing in vacuum. Sintering particles make contact by fusion of the vitreous or semi-molten surface layer. (Scale bars both 10 μm.) (b) Crushed d-$LiKC_4H_4O_6.H_2O$ after dehydration at 423 K started with 1050 Pa of initial water vapour. (Scale bar 100 μm.)

boundary, with rounded rather than sharp textural features, is indicative of control by surface tension rather than crystallographic forces.

The textures of product after seven successive dehydrations ($\alpha = 1.00$ at 423 K) and rehydrations (to $\alpha = 0$ at *ca.* 290 K) are shown in figure 15a, b. The outer boundary surface was coherent, smooth and penetrated by numerous channels of diameters 0.5–5 μm, figure 15a. The internal texture, revealed by cleavage, figure 15b, showed the residual product to be composed of small crystallites, typically 1–2 μm diameter, and the mass is penetrated by channels 1–3 μm diameter.

PHILOSOPHICAL TRANSACTIONS OF THE ROYAL SOCIETY A MATHEMATICAL, PHYSICAL & ENGINEERING SCIENCES
PHILOSOPHICAL TRANSACTIONS OF THE ROYAL SOCIETY A MATHEMATICAL, PHYSICAL & ENGINEERING SCIENCES

Downloaded from rsta.royalsocietypublishing.org

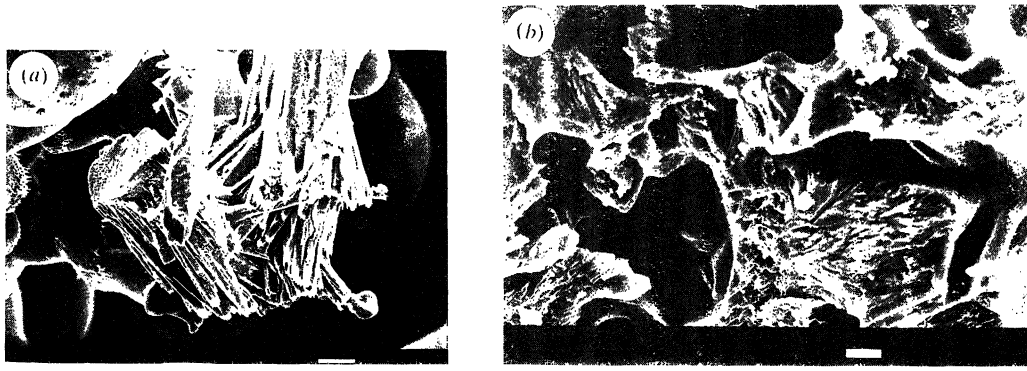

Figure 17. Centre of *d*-$LiKC_4H_4O_6.H_2O$ crystallites after dehydration ($\alpha = 1.0$ at 423 K). Textures of the product particles composing the nuclei are similar to those found in single crystals (figures 3–4). (Scale bars both 10 μm.)

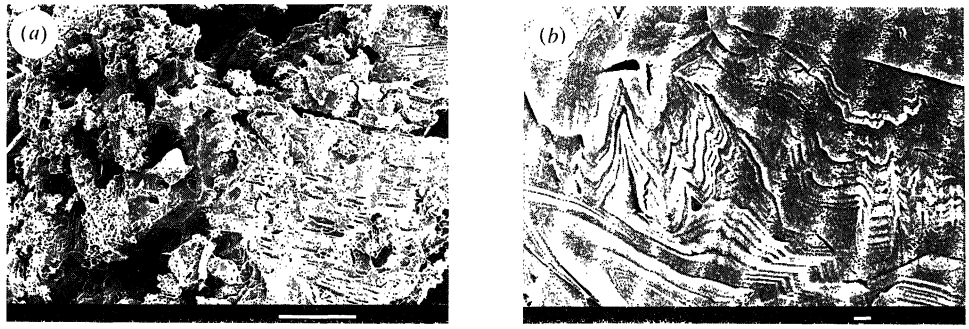

Figure 18. Powdered *d*-$LiKC_4H_4O_6.H_2O$ after dehydration ($\alpha = 1.00$ at 463 K). Textures of product salt are similar to those found in single crystals dehydrated at relatively higher temperatures (figure 10*a*, *b*). There is evidence of extensive sintering of the recrystallized outer surface. (Scale bar: (*a*) 100 μm; (*b*) 1.0 μm.)

The dehydration of crushed crystal reactant

The most obvious textural feature of the dehydrated crushed crystals (mean particle size *ca.* 120 μm) was the extensive sintering of crystallites that occurred during reaction, yielding product ($\alpha = 1.00$) in the form of hard coherent aggregates. Samples of crushed salt dehydrated at 423 K, commencing in vacuum and in *ca.* 1050 Pa water vapour, are shown in figure 16*a*, *b*. Interparticle contracts were apparently generated during sintering of the vitreous or semi-molten surface layer; the typically rounded features are seen at higher magnification in figure 16*c*. This is a principal reason for our conclusion that this superficial layer is a viscous fluid or a semi-molten vitreous phase at reaction temperature. Obtaining a photographic record of the structures of the centres of these small particle proved difficult, due to sample deterioration in the microscope beam at the relatively high magnifications required. Textural features already described in figures 3 and 4 were also observed visually for powders in figure 17*a*, *b* ($\alpha = 1.00$ at 423 K). This is evidence of the occurrence here of the nucleation and growth reaction, the dominant reaction of crystals, during the later stages of powder dehydrations ($\alpha > 0.5$, see figure 2). Similarly, the different internal texture, characterized above for high temperature

Downloaded from rsta.royalsocietypublishing.org

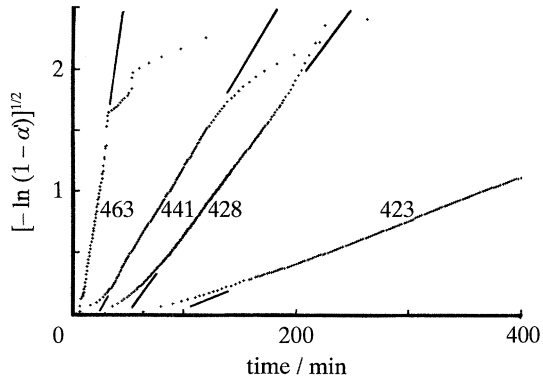

Figure 19. Representative plots for the isothermal dehydrations of single crystals of *d* lithium potassium tartrate monohydrate to show the fit of the Avrami–Erofe'ev equation: $[-\ln(1-\alpha')]^{\frac{1}{2}} = kt$. Data from same experiments as in figure 1 (α_i values subtracted).

(more than 460 K) dehydrations, is again found in the product of powder dehydration ($\alpha = 1.00$) at 463 K, figure 18*a*. There is also evidence of more extensive sintering during recrystallization of the outer surface of the same aggregated specimen, figure 18*b*.

4. Kinetics of second reaction for single crystal dehydrations

(*a*) *Rate characteristics and reproducibility*

Fractional reaction α–time curves for the second reaction during the isothermal dehydration of *d* lithium potassium tartrate monohydrate (DLKTM) were sigmoidal (figure 1). After subtracting individual contributions due to the first reactions ($\alpha_i = 0.03 < \alpha < 0.04$), data were very satisfactorily fitted by the Avrami–Erofe'ev equation, $n = 2$ (figure 19).

$$[-\ln(1-\alpha')]^{\frac{1}{2}} = kt, \tag{1}$$

where $\alpha' = (\alpha - \alpha_i)/(1.00 - \alpha_i)$. Fits were equally satisfactory for $n = 2$, 2.5 and 3 and it was found convenient to use the $n = 2$ form as the most acceptable basis for kinetic comparisons.

This kinetic conclusion is consistent with the microscopic evidence that dehydration is a nucleation and growth process. The growth of three-dimensional compact nuclei is expected (Brown *et al.* 1980) to result in obedience to the $n = 3$ expression. However, the present behaviour is, at least qualitatively, reconciled with this model by the observation that nuclei were not hemispherical but flattened and irregular in outline. Furthermore, nuclei were not randomly distributed but appeared preferentially at edges and corners on reactant particles (40–50 mg crystals) that were cuboid rather than cubic. All these parameters exert some influence on the kinetic characteristics of this rate process controlled by geometric factors.

Reaction rates differed appreciably for successive similar experiments. Accordingly, to characterize reproducibility, 30 dehydrations were measured under identical conditions at 423 ± 2 K. Induction periods for the second reaction, defined as the time required to reach the $(d\alpha/dt)$ minimum value between the two rate processes, were 50 ± 15 min. Rate constants, values of k in equation (1), showed a mean variation of $\pm 30\,\%$ (between extreme values $\pm 60\,\%$). This range of variation can be expected as a result of differences in the small (non-statistical) numbers of

Downloaded from rsta.royalsocietypublishing.org

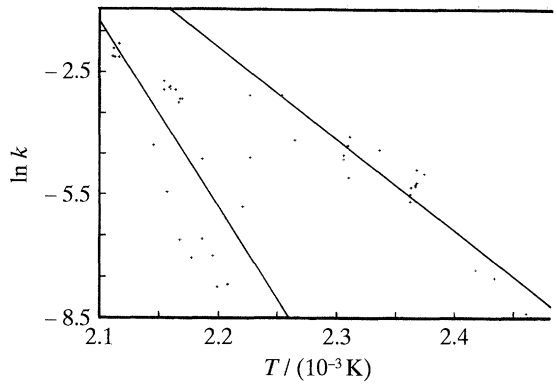

Figure 20. Arrhenius plot for dehydration of single crystals using Avrami–Erofe'ev equation ($n = 2$) rate constants. For discussion see text.

nuclei, often less than 20, irregularly disposed on the reactant crystals. Most reaction rates were within limits ($\times 2$) that can be readily envisaged as arising where nucleation is predominantly on one side of the crystal only or where nuclei are distributed randomly across all crystal faces.

(*b*) *Influence of temperature on crystal dehydrations*

The pattern of the typical α–time plots shown in figure 1 represents a simplification of the behaviour characterized by our kinetic studies in two important respects. First, magnitudes of rate constants showed the significant scatter (*ca.* $\times 2$) discussed above. Secondly, increase of reaction temperature resulted in an increase in dehydration rate between 390 K and 445 K but above this temperature there was a marked decrease in rate before further increases in the range 453–473 K. Both effects are clearly seen in the Arrhenius plot for equation (1) rate constants, figure 20. It is convenient, therefore, to discuss kinetic characteristics in two temperature intervals that also correspond to the two different nucleus textures distinguished in the electron microscopic observations discussed above.

390–443 K

α–time data satisfactorily fitted equation (1) ($0.05 < \alpha < 0.95$) and rate constants gave Arrhenius parameters, calculated by linear regression analyses: activation energy, 175 ± 30 kJ mol^{-1} and frequency factor, 3.8×10^{20} min^{-1}.

453–473 K

Reaction rates above 453 K were significantly slower than those at lower temperatures, shown by the comparison in figure 21. These α–time plots were only approximately sigmoidal, gas evolution typically proceeded through a sequence of spasmodic evolutions, often 2 to 5, giving appreciable fluctuations in rates of water release. Data, however, obeyed equation (1) sufficiently closely to enable these rate constants to be used for kinetic comparisons. Moreover, the electron micrographs (e.g. figure 9) confirm the operation of nucleation and growth mechanism, though the intranuclear textures in this higher temperature range differ from those observed for reactions at lower temperatures. Arrhenius parameters, calculated by linear regression analyses for the appreciably scattered values, were: activation energy, 350 ± 50 kJ mol^{-1} and frequency factor, 1.9×10^{40} min^{-1}, figure 20.

Downloaded from rsta.royalsocietypublishing.org

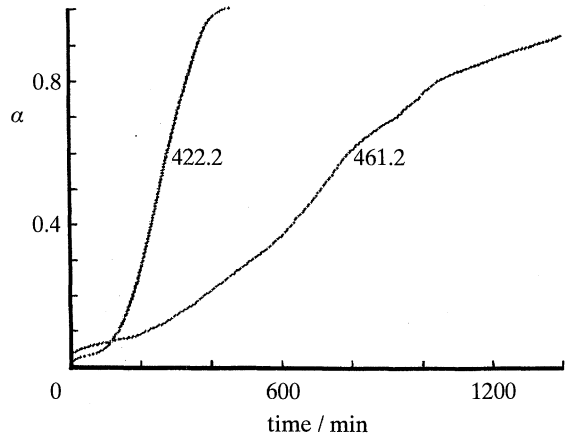

Figure 21. Comparative α–time plots for dehydrations of single crystals at two temperatures. The low temperature reaction (422.2 K) exhibited the sigmoid shape curve characteristic of the nucleation and growth reaction. At the higher temperature (461.2 K) the reaction was significantly slower and kinetic behaviour more irregular, exhibiting intermittent changes of rate.

In this higher temperature range, the extent of the first reaction increased somewhat, sometimes to *ca.* 10% (figure 21). During the extended times required for completion, there was evidence of the onset of decomposition and up to 3% of a product, identified as CO_2 (Galwey & Laverty 1993), remained uncondensed in the presence of a 213 K trap. The residual solid products were white, cracked crystals that included local brown coloured zones (probably due to local decomposition).

(*c*) *Effect of preadmitted water vapour on crystal dehydrations at 423 K*

Pressures of water vapour of 60–1000 Pa were admitted to the reaction vessel before individual kinetic measurements. This increased the rate and the extent of the first reaction, as described in part I. Rate constants for the second reaction were not, however, significantly different from those of otherwise identical reactions initiated in vacuum. We conclude that low pressures of preadmitted water vapour exert no appreciable influence on dehydration kinetics of the second reaction, except for a small reduction (*ca.* 25%) in the induction period.

(*d*) *Dehydration of crystal in contact with dehydrated powder at 423 K*

In these experiments, each DLKTM crystal (*ca.* 30 mg) was surrounded in the reaction vessel by a similar mass of crushed, previously dehydrated ($\alpha = 1.00$) powder. A typical α–time plot for the reaction of this combination is compared with the dehydration of a single crystal in figure 22. The presence of the product results in marked increases in both rate ($\times 100$) and extent ($\alpha_i = 0.10$) of the first reaction. The induction period for the second reaction is reduced from 50 min to 15 min, the acceleratory phase was almost eliminated and the deceleratory kinetic behaviour obeyed the contracting volume expression (Brown *et al.* 1980). We conclude, therefore, that product–reactant contacts promote the early establishment of an active interface over all surfaces, causing an increase in reaction rate and change of the kinetic expression obeyed. This is ascribed to contact of the dehydrated surface of the reactant with the product crystalline phase which acts as superficial seed crystals, thus eliminating the delay that is otherwise required for nucleation, the generation of recrystallized product.

PHILOSOPHICAL TRANSACTIONS OF THE ROYAL SOCIETY A MATHEMATICAL, PHYSICAL & ENGINEERING SCIENCES
PHILOSOPHICAL TRANSACTIONS OF THE ROYAL SOCIETY A MATHEMATICAL, PHYSICAL & ENGINEERING SCIENCES

Downloaded from rsta.royalsocietypublishing.org

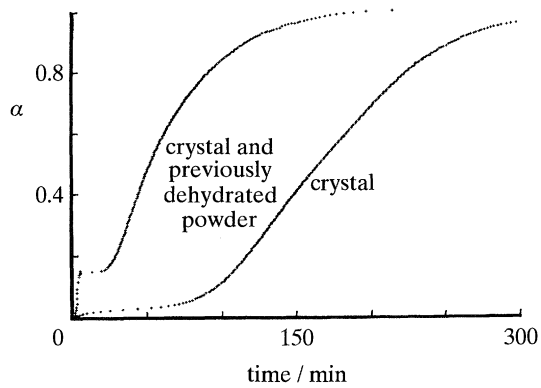

Figure 22. Comparative α–time plots for dehydrations of single crystals at 422 K. The addition of dehydrated powder, the crystalline anhydrous product of reaction, markedly reduced the induction period to onset of reaction and accelerated the rate of the subsequent dehydration compared with the reaction of a crystal without additive.

It is interesting to note further that powdered dehydrated *d* dipotassium tartrate was similarly effective in reducing the induction period in DLKTM dehydration and again the contracting cube obedience was found. This related salt is similarly capable of promoting extensive superficial nucleation.

(*e*) *Dehydration/rehydration cycles at 423 K*

A selected crystal of good habit, 36 mg, was subjected to a sequence of seven successive dehydration rate measurements, each followed by rehydration at 290 K in saturated water vapour. Kinetic characteristics for all these experiments were as expected for a nucleation and growth process. Induction periods for second and subsequent dehydrations were, however, short. Rate constants, k values for equation (1), increased to a constant value during cycles 1–5 in the ratio 1.0:1.2:3.5:4.0:5.0:5.0:5.0. The rise in reactivity may be ascribed to an increase in effective active surface area of the reactant, retextured (figure 14*a*, *b*) as a consequence of each dehydration/rehydration cycle and which presumably reaches a limiting value. These data, with mass measurements, confirm that the loss of the water of crystallization is reversible, providing that rehydration occurs at the lower temperature.

(*f*) *Dehydration of reactant pellet at 423 K*

Each reactant pellet was a compact, coherent disc prepared by compression of crushed powder at 80 kN m^{-2} for 5 min.

The kinetic characteristics of DLKTM pellet dehydration at 423 K were intermediate between those of crystals and powder, figure 23. Behaviour may be interpreted as that of an adherent assemblage of small crystals permeated by an extensive system of channels that permit the escape of product water. The extent of the first reaction (33%) was somewhat less than that for powder reactants and the induction period was similar to that for a single crystal (*ca.* 50 min). The second reaction was sigmoidal, equation (1) was again applicable and the dehydration rate was about twice that for the single crystal.

Downloaded from rsta.royalsocietypublishing.org

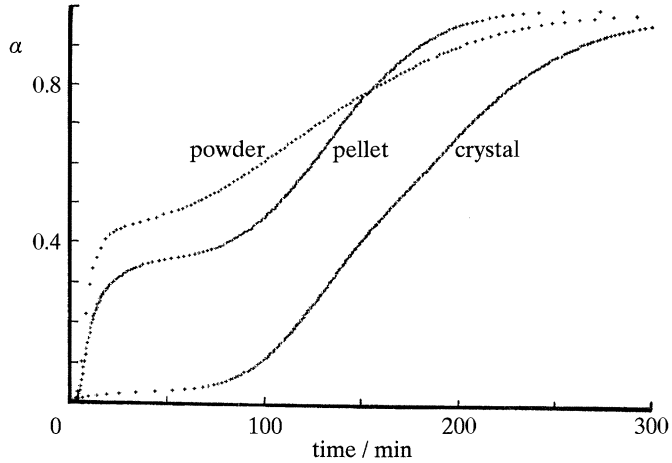

Figure 23. Comparative α–time plots for dehydrations, at 423 K, of three forms of reactant: single crystal, crushed crystals and powder compacted to form a coherent pellet.

5. Kinetics of the second reaction for crushed powder dehydrations

(*a*) *Rate characteristics and reproducibility*

Representative α–time curves for dehydrations of crushed crystals of DLKTM across the temperature interval of the present kinetic studies are shown in figure 2. The increased yield from the first reaction, to $\alpha = 0.3$–0.4, is ascribed to the much larger aggregate surface area of the reactant, compared with crystals, and has been discussed in part I. The subsequent sigmoidal curve is the nucleation and growth second reaction.

The kinetics of crushed crystal dehydrations were appreciably more reproducible than the behaviour of crystals described above. This is ascribed to the elimination of crystal inhomogeneities and relaxation of local stresses during crushing, thereby producing an assemblage of crystallites with relatively more homogeneous reactivities. Elimination of those sites of greatest reactivity also explains the observed small average rise in induction period from crystal to powder (50–75 min) at 423 K.

(*b*) *Kinetics of dehydration of crushed crystals*

The sigmoidal portion of the α–time curves for the second reaction obeyed equation (1), again with $n = 2$, after subtraction of the contribution from the first reaction. The mean rate constant (equation (1)) for dehydration of crushed powder (including a range of particle sizes) at 423 K was $5.2 \pm 1.7 \times 10^{-3}$ min^{-1} (representing $0.45 < \alpha < 0.95$) and this is in excellent agreement with the mean value for single crystals, $5.3 \pm 3.0 \times 10^{-3}$ min^{-1}. The results of more detailed investigations of the variation of dehydration rates with crystallite sizes, using sieved samples of salt, are summarized in table 1.

Variation of particle sizes

Dehydrations of the finest crystals, (edges < 125 μm, table 1 and figure 24) resulted in the evolution of more than 70% of the constituent water in the first reaction. No evidence of the occurrence of a second reaction could be obtained when $\alpha > 0.7$. This suggests that nucleus formation does not occur in the finely divided, strongly cold worked smallest crystallites.

Downloaded from rsta.royalsocietypublishing.org

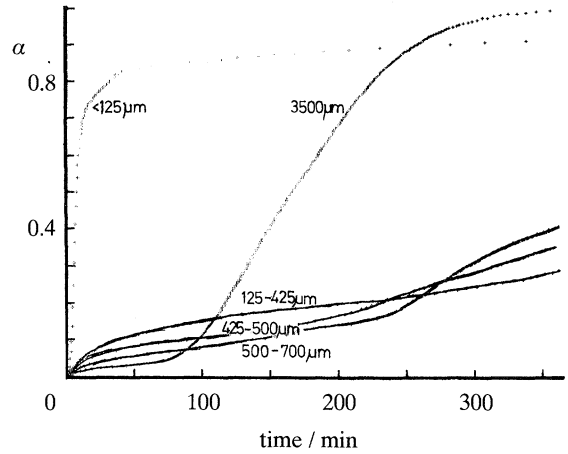

Figure 24. Comparative α–time plots for the isothermal (423 K) dehydrations of finely crushed powder (< 125 μm), single crystal (3.5 mm edge) and three samples of powder graded in intermediate size ranges, see also table 1. For discussion see text.

Table 1. *Influence of particle size on dehydration of* d-*lithium potassium tartrate monohydrate at 423 K*

particle size (crystal edge/μm)	< 125	125–425	425–500	500–700	3500
completion of first reaction (α_i)	0.7	0.20	0.11	0.07	0.03
estimated thickness of dehydrated layer on completion of first reaction/μm	11	7	9	7	10
induction period to second reaction/min	—	208	120	75	50
rate coefficient, $k/(10^{-3}\ \mathrm{min}^{-1})$	—	2.1	20.1	21.3	5.3

In the other three sieved powder fractions, crystallite sizes 125–425, 425–500 and 500–700 μm (table 1 and figure 24), the extent of the first reaction, as measured by α_i, increased with surface area of the reactant but the estimated thickness of the dehydrated layer was more nearly constant. Induction periods to onset of the second reaction also increased with decrease in crystallite size. This is ascribed to the elimination, by particle disintegration and cold working, of the inherently most active specialized imperfections that are identified as the essential precursors to nucleus formation. The second reaction obeyed equation (1) with $n = 2$. Although there were appreciable variations in reactivity of individual reactant crystals, the dehydration rates of powders were similar to those of single crystals.

Mixture of hydrated and dehydrated crushed powder

The role of the recrystallized product in initiating reaction was investigated by measuring the dehydration rates of a mixture of crushed crystals (particle edges *ca.* 120 μm) with previously dehydrated powder that had been subsequently lightly crushed. The reaction at 423 K was relatively rapid. Dehydration proceeded to completion in a deceleratory process, identified as the second reaction, that obeyed the contracting volume equation (Brown *et al.* 1980) between $0.04 < \alpha < 0.91$ and

Downloaded from rsta.royalsocietypublishing.org

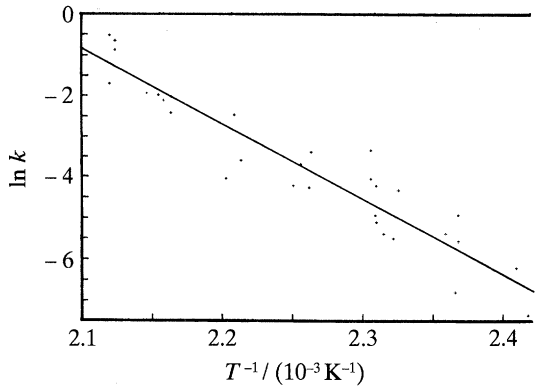

Figure 25. Arrhenius plot for second reaction in powder dehydrations, using rate constants from equation (1) after subtraction of the contribution from the first reaction.

was 95% completed in 30 min. This is strong evidence that the product effected initial rapid and dense nucleation within the hydrate crystallites. The interface of reactant-recrystallized product thus generated across all particle surfaces advanced thereafter into crystallite interiors.

Influence of temperature on crushed powder dehydrations

Onset times for the second reaction decreased somewhat with increasing reaction temperatures (figure 2) and there was evidence of a small amount of decomposition during reactions above 460 K, representing a 1–2% yield of CO_2.

Following the induction period, 400 min at 413 K decreasing to 90 min at 443 K, the second reaction exhibited the sigmoid α–time curve. This process obeyed equation (1), after subtraction of the contribution from the first reaction, and exponents (n) giving the best fit varied between 2 and 4 for individual experiments. Again the $n = 2$ fit provided a sufficiently acceptable obedience to be used as a basis for kinetic comparisons but rate data from the highest temperature experiments (more than 445 K) were less reliable. From linear regression analysis of the Arrhenius plot (figure 25, rate constants from equation (1)), the calculated values were: activation energy, 153 ± 10 kJ mol^{-1} and frequency factor 2.5×10^{16} min^{-1}.

Effect of preadmitted water vapour on crushed powder dehydrations at 423 K

Representative α–time plots for crushed powder dehydrations at 423 K are shown in figure 26 for reactions in the various specified pressures of preadmitted water vapour. This additional water vapour markedly increased, but did not systematically vary, the induction period to the second reaction. The rates of the final stages of the first reaction have been diminished but the rates of the second reaction are essentially unchanged. For the same crushed powder reactant, the rate constants (equation (1)) are between $2.2–3.1 \times 10^{-3}$ min^{-1} when water vapour was present and 3.8×10^{-3} min^{-1} for vacuum initiated reaction. We conclude, therefore, that the 'excess' water present inhibits the essential steps that culminate in the recrystallization that is required to form a stable nucleus. These controls result in the relatively complex pattern of behaviour seen in figure 26 and the reasons have not been completely elucidated from the data available.

PHILOSOPHICAL TRANSACTIONS OF THE ROYAL SOCIETY A MATHEMATICAL, PHYSICAL & ENGINEERING SCIENCES
PHILOSOPHICAL TRANSACTIONS OF THE ROYAL SOCIETY A MATHEMATICAL, PHYSICAL & ENGINEERING SCIENCES

Downloaded from rsta.royalsocietypublishing.org

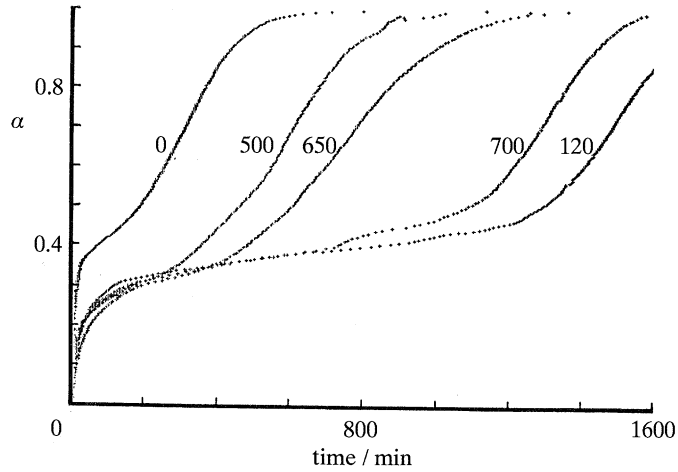

Figure 26. α–time plots for powder dehydrations at 423 K in the various specified pressures of preadmitted water vapour (values in Pa). Water present before reactant heating delayed the onset of reaction but no systematic trend was discerned.

Table 2. *Summary of kinetic and Arrhenius data for dehydrations of lithium potassium tartrate hydrates*: d, dl *and* meso *forms of the anion*

salt	form	reaction	ln[k(425 K)/ min^{-1}]	ln[k(465 K)/ min^{-1}]	activation energy/ (kJ mol^{-1})	frequency factor/ min^{-1}
d	crystal	first	-21.2 cm^2 s^{-1}	-17.3 cm^2 s^{-1}	155 ± 4	5×10^8 cm^2 s^{-1}
d	powder	first	-21.7 cm^2 s^{-1}	-17.6 cm^2 s^{-1}	153 ± 8	3×10^8 cm^2 s^{-1}
d	crystal	second < 460 K	-5.2	-1.0[a]	175 ± 30	3.8×10^{20}
d	powder	second	-5.5	-1.7	153 ± 10	2.5×10^{16}
d	crystal	second > 460 K	-13.2[a]	-3.7	350 ± 50	1.9×10^{40}
dl	crystal	zero order	-9.4	-1.4	330 ± 20	8.7×10^{36}
dl	powder	zero order	-7.0	$+0.5$[a]	312 ± 30	6.3×10^{36}
meso	crystal	zero order	6.4[a]	12.1[a]	230 ± 10	2.5×10^{31}
meso	powder	zero order	7.5[a]	13.2[a]	230 ± 10	7.5×10^{31}

[a] Extrapolated value.

6. Arrhenius parameters

Arrhenius parameters for the first and second reactions in the dehydration of lithium potassium tartrate hydrates, the *d* salt and the main dehydrations of the *dl* salt (Bhattamisra *et al.* 1992) and *meso* (Galwey *et al.* 1992) salt, are compared in table 2. The initial rates of *d* salt crystal dehydrations measured in this study were appreciably irreproducible and the magnitudes given in the first row (table 2) were from Galwey & Okhotnikov (1988) using data that were in the median region of the band of more scattered values obtained during the present kinetic measurements. Rate constants for the second reaction (less than 460 K) of the *d* salt crystals were similarly scattered, as reflected in the large uncertainty recorded for the activation energy (175 ± 30 kJ mol^{-1}).

Two general features emerge from comparison of the data in table 2.

(i) Dehydration rates and activation energy magnitudes for both first and second

Downloaded from rsta.royalsocietypublishing.org

reactions and for both crystals and powders of the *d* salt are closely similar. We conclude that the activation energy for the dehydration of DLKTM (at less than 460 K) is 150–160 kJ mol^{-1}.

(ii) Rate constants and Arrhenius parameters for the high temperature (more than 460 K) dehydration of the *d* crystals compare well with data for both crystal and powder dehydrations in the main (zero order) reaction of the *dl* salt (Bhattamisra *et al.* 1992). This reaction has been identified as occurring in a melt.

7. Mechanism of the dehydration of *d* lithium potassium tartrate monohydrate

This mechanistic discussion is concerned with the dehydration of the *d* salt, considering together the relations between both first and second reactions. The early part of the first reaction has already been identified (part I) as being controlled by migrations of H_2O molecules within a developing and increasingly disordered vacancy structure. Later this becomes so extensively disordered that it is transformed into a superficial vitreous or possibly a molten layer. The significant change that characterizes the establishment of the second reaction is the appearance of the crystalline anhydrous product, figures 3–5 (Baranov *et al.* 1990). This essential structural reorganization underlies our mechanistic interpretation of the results. Crystalline product is generated during nucleation, and growth is the advance of the boundaries encompassing these crystalline aggregates of anhydrous product, explaining the characteristic sigmoidal α–time curves for the second reaction. Initiation of the recrystallization of the water depleted product to the anhydrous salt is identified as the difficult step, a conclusion that has close similarities with that previously proposed for alum dehydrations (Galwey *et al.* 1981, Galwey & Guarini 1993). Nucleation in partly dehydrated $Na_2S_2O_3.5H_2O$ has been discussed by Guarini & Piccini (1988).

8. Nucleation

The microscopic evidence shows that nuclei are formed at or near surfaces, consistent with the requirement that the released product water can escape from the active reaction zones. Observations also suggest that recrystallization does not texturally modify the outer boundary layers of the crystal that have undergone the most extensive water depletion during the first reaction (figure 8). It appears most probable, therefore, that nuclei are formed at, or near, the inner limit of the dehydration zone of the first reaction, beneath the extensively modified surface. The difficulties in characterizing the nature of the specific nucleation sites involved are considerable because relatively few (*ca.* 20) sites exist on our crystal reactants (edge *ca.* 3 mm). This infrequency of occurrence of such sites suggests that each may be a combination of structural imperfections. Because these become active within a zone of water loss, local strains may influence the ionic movements whereby the germ crystal possessing the structure of the product appears. This cooperative model is more complicated than the sometimes highly localized events that are often envisaged in nucleation theory (Garner 1955; Brown *et al.* 1980).

The product of the first reaction is an effective barrier to continued water escape. The significant feature of the second reaction is the ability of the recrystallization step to open channels of water escape that are an essential prerequisite to nucleus growth. Product structure generation is identified, therefore, as a consequence of the

PHILOSOPHICAL TRANSACTIONS OF THE ROYAL SOCIETY A MATHEMATICAL, PHYSICAL & ENGINEERING SCIENCES
PHILOSOPHICAL TRANSACTIONS OF THE ROYAL SOCIETY A MATHEMATICAL, PHYSICAL & ENGINEERING SCIENCES

Downloaded from rsta.royalsocietypublishing.org

bond redistributions at specialized structural imperfections within the stress field of the advancing dehydration zone of the first reaction. This nucleation model is consistent with the following observations.

(i) The nucleation process is slower in crushed crystals than in single crystal reactants. Mechanical cold working during grinding can be expected to destroy crystal imperfection structures (Sheen & Sherwood 1985). The effect of removal of potential nucleation sites more than offsets the increase of reactant area across which reaction may be initiated. The finest of the reactant powders (less than 125 μm) apparently generated no nuclei (see table 1).

(ii) The evidence most strongly linking nucleation with the generation of product crystalline phase was the observation that the induction period was effectively eliminated in mixtures already containing anhydrous crystalline product: (crystals + dehydrated salt) and (powder + dehydrated salt). Indeed, the transformation from a sigmoidal α–time curve to the overall deceleratory obedience, characteristic of the contracting volume model, by covering crystal with product powder, demonstrates convincingly the effectiveness of these 'seed crystals' in initiating the second reaction. The first reaction was effectively suppressed in reactions of powder-with-product mixtures. Similarly, in dehydrations of rehydrated salt, the second reaction was initiated without delay (the induction period at 423 K was reduced from 53 to less than 8 min), suggesting the retention of material containing features of the product structure after exposure to water vapour.

(iii) Water vapour, admitted to the apparatus before the initiation of reaction, reduced the induction period for the second reactions in crystals by *ca.* 25%, whereas for powder it was somewhat increased. It is known that water vapour modifies product layer textures (figure 13*a*), presumably also influencing vacancy concentrations and their distribution during the first reaction. It must be concluded here that this influence of imperfections in large crystals is different from that exerted on the possibly different types of imperfections remaining after cold-working in crushed powder particles.

9. Growth

Less than 450 K. Growth is the crystallization of extensively, or completely, dehydrated material at the boundary of, and augmenting, the crystalline anhydrous product aggregate that constitutes each nucleus. Such reorganization of dehydrated material is promoted by the product phase present, and recrystallization opens channels permitting water loss from the hydrate layer so exposed by the diffusive escape mechanism described for the first reaction. Advance of the recrystallization boundary is probably spasmodic, irregular in space and time, giving nuclei the serrated outlines seen in figures 3 and 4. Figure 4 indicates that close contact of product with the reactant is essential for the maintenance of growth which has evidently, in this example, been much more effective on one side than on the other of the crack that is the channel of water vapour escape.

The identification of interface advance with continued regeneration of the first reaction at the boundary of an advancing growth nucleus is confirmed by the following quantitative comparison. The dehydration rates reported above show that, at 423 K, single crystals of edge *ca.* 3 mm complete this reaction in 200–400 min (subtracting the contribution from the first reaction). This range of reaction rates ($\times 2$) is ascribed to variations in the dispositions of the small number of nuclei, perhaps on one side only (400 min reaction time) or perhaps on both sides (200 min)

PHILOSOPHICAL TRANSACTIONS OF THE ROYAL SOCIETY A MATHEMATICAL, PHYSICAL & ENGINEERING SCIENCES
PHILOSOPHICAL TRANSACTIONS OF THE ROYAL SOCIETY A MATHEMATICAL, PHYSICAL & ENGINEERING SCIENCES

Downloaded from rsta.royalsocietypublishing.org

of a reactant crystal. From these data we conclude that the mean rate of interface advance is $3000/400 = 1500/200 \approx 7\ \mu m\ min^{-1}$. This agrees closely with the dehydration rate recorded for the first reaction at the point of transition from region II to region III (the sustained reaction) listed in table 1 (part I) at 423 K (92×10^{-7} cm s^{-1}) = 5.5 μm min^{-1}. The rate constant concerned specifies the transition of water molecules from the chemically bound state to the free state (see part I). Thus water is lost from the inner zone of the active interface by diffusive escape from the reactant structure, but regular crystallization of the product layer is required to regenerate surfaces capable of sustaining such loss. This model explains the following two observations.

(i) The rates of single crystal and of crushed crystal dehydrations were closely similar. The capacity of added product phase (seed crystals) to initiate sustained dehydration is evidence of the ability of product crystallization to traverse intercrystalline contacts. It follows, therefore, that during powder dehydrations, nuclei generated on one particle can advance into neighbours and thus the interfaces present are able to progress throughout the crystallite mass. This may be assisted by the interparticular sintering that occurs during the first reaction in the powder. Consequently, once nuclei have been generated in a powder assemblage, the time taken to complete dehydration is comparable with that for the reaction of a crystal of similar dimensions because the interfacial advance processes are identical. Moreover, since such nuclei can be generated at crystallites within the aggregate of powder (rather than at boundary surfaces only of crystals) the kinetic behaviour is expected to be more reproducible.

(ii) Activation energies for the first and second reactions, for both crystals and powders, are identical (150–160 kJ mol^{-1}). This is to be expected if the controlling steps of the first reaction determine the rate of the second. We also note that this value is very much larger than the dehydration enthalpy, measured during the present work as 45 ± 5 kJ mol^{-1}.

More than 450 K. A most significant textural feature of the product nuclei developed during these dehydrations was the rounded boundary surfaces, indicative of melt formation and surface tension control (figures 9 and 10). The characteristic crystallite textures of the lower temperature reaction were not present, the coherent product assemblages here were relatively much larger. By analogy with the tendency for superficial layers of salt to undergo melting, we conclude that the melting point of the partly dehydrated salt has been reached during these reactions. Nucleation and growth behaviour is maintained due to the presence of product anhydrous phase in the nuclei and the consequent volume diminution on recrystallization opens escape channels for water losses. The rate of dehydration of the liquified, partly dehydrated salt is controlled by factors applicable to molten reactant and kinetic characteristics are comparable with those measured for dehydration for the *dl* salt (Bhattamisra *et al.* 1992, see also table 2 above). This mechanism differs from the solid state reaction described above (< 450 K) only in identifying the role of a relatively thicker liquid interfacial layer from which water is released under kinetic controls that are different from those applicable to the first reaction proceeding in the disorganized water site vacancy structure of the reactant solid. Again, promoted recrystallization of the solid product (anhydrous salt) maintains the growth of nuclei.

PHILOSOPHICAL TRANSACTIONS OF THE ROYAL SOCIETY A MATHEMATICAL, PHYSICAL & ENGINEERING SCIENCES
PHILOSOPHICAL TRANSACTIONS OF THE ROYAL SOCIETY A MATHEMATICAL, PHYSICAL & ENGINEERING SCIENCES

Downloaded from rsta.royalsocietypublishing.org

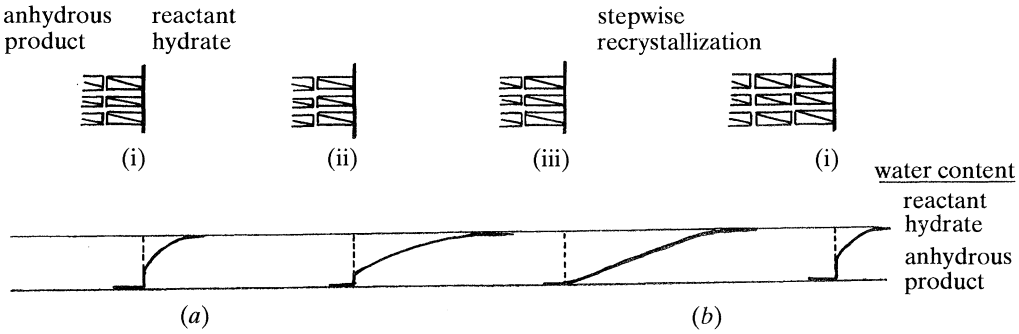

Figure 27. Structure and water losses within an advancing reaction interface (relation between first and second reactions).

(*a*) Water is lost from the zone of hydrated reactant adjoining an advancing active reaction interface that is the boundary of the nucleus. Water loss is by the mechanism of the first reaction. This is deceleratory, diffusive escape of H_2O from the disordered structure of the hydrate reactant.

(*b*) Recrystallization of the water depleted zone exposes new surfaces capable of further water loss. Continued regeneration of the reaction zone maintains interface advance by removal of the inhibitory effect of first reaction product accumulation. Product reorganization opens channels for water escape and the first reaction mechanism is applicable to advance of the nucleus boundary during the second reaction.

Recrystallization is the difficult step but once growth nuclei are established the inhibitory character of the first reaction is suppressed. The four diagrams shown above represent, at increasing times, the interface (vertical bar) between recrystallized anhydrous product (rectangles on left of bar) and dehydrating salt which progressively looses water as represented by the graphs below each diagram. When dehydration has sufficiently advanced (third diagram) recrystallization of water depleted material results in a spasmodic interface advance, promoted by contact with the crystalline product which facilitates the necessary structural reorganization.

10. The surface layer

Microscopic evidence (figures 5, 6, 9 and 11) identifies the outer dehydrated surfaces of crystals as vitreous and probably molten material. Powder reactant crystallites form coherent aggregates by sintering during the first reaction (figure 16). The presence of water vapour, admitted before dehydration experiments, promoted surface textural reorganization (figure 13) and influenced kinetic behaviour. We conclude, therefore, that a proportion of water vapour is retained within and modifies the properties of the partly dehydrated outer zone developed during diffusive losses from the unrecrystallized salt. Accommodation of water within the product of the first reaction, extending across the outside faces of nuclei, may enhance plasticity and so generate the bubbles that are seen during dehydrations (figure 9*c*, *d*).

Unlike alums (Galwey *et al.* 1981), however, water vapour present before initiating dehydration does not promote nucleation or crystallization of DLKTM, because it is relatively less readily condensed at the present higher reaction temperatures and is expelled from the nuclei more readily.

11. Conclusions

The mechanism proposed accounts very satisfactorily for both kinetic and microscopic observations. We conclude that the initial water release is from all reactant crystal surfaces. This is diffusion controlled and proceeds in a changing

PHILOSOPHICAL TRANSACTIONS OF THE ROYAL SOCIETY A MATHEMATICAL, PHYSICAL & ENGINEERING SCIENCES
PHILOSOPHICAL TRANSACTIONS OF THE ROYAL SOCIETY A MATHEMATICAL, PHYSICAL & ENGINEERING SCIENCES

Downloaded from rsta.royalsocietypublishing.org

vacancy structure of the increasingly disorganized reactant crystal. Reaction rate is deceleratory and diminishes to a low value. Subsequent generation of small numbers of crystallites of the anhydrous product phase has the effect of introducing seed crystals from which reaction strongly propagates as growth of three-dimensional nuclei composed of crystalline anhydrous product. At the active nucleus boundary, the advancing interface is composed of a reactant surface layer from which water is lost by the diffusion mechanism. When this has proceeded sufficiently, the water depleted block is transformed into the product structure by contact with product crystallites already present (figure 27). This recrystallization opens channels for water escape from which newly exposed hydrate surfaces initiate further water loss and so growth is maintained by intermittent interface advance. Evidence was also obtained to indicate that recrystallization is capable of propagation from one crystallite to a neighbour touching it. Dehydration rates of single crystals and aggregates of powder having similar dimensions react at similar rates.

The rate controlling factor in this reaction is, therefore, identified as the loss of water by the diffusion process (first reaction). However, the most difficult step in initiating the second reaction is product recrystallization, but once this has been achieved the dehydration is capable of sustained propagation, enabling the self-inhibiting diffusion deceleratory process of the first reaction to regenerate continually. We conclude, therefore, from the kinetic and microscopic evidence that the two types of dehydration distinguished in the introduction both participate in the mechanism proposed for water release from DLKTM.

One of us (G.M.L.) thanks the Department of Education for Northern Ireland for the award of a Postgraduate Scholarship (CAST Award) held during the period of this work. We thank Mr J. McCrae and the Staff of the Electron Microscope Unit (QUB) for help and advice in obtaining the electron micrographs.

References

Baranov, N. A., Okhotnikov, V. B., Rynskaya, L. I., Semenov, A. R., Galwey, A. K. & Laverty, G. M. 1990 *Solid State Ionics* **43**, 37.

Bhattamisra, S. D., Galwey, A. K., Laverty, G. M. & Okhotnikov, V. B. 1992 *Phil. Trans. R. Soc. Lond.* A **341**, 479.

Boldyrev, V. V., Gapanov, Y. A., Lyakhov, N. Z., Politov, A. A., Tolochko, B. P., Shakhtshneider, T. P. & Sheromov, M. A. 1987 *Nucl. Inst. Method. Phys. Res.* A **261**, 192.

Brown, M. E., Dollimore, D. & Galwey, A. K. 1980 *Comprehensive chemical kinetics*, vol. 22. Amsterdam: Elsevier.

Carr, N. J. & Galwey, A. K. 1986 *Proc. R. Soc. Lond.* A **404**, 101.

Galwey, A. K. 1985 *Thermochim. Acta* **96**, 259.

Galwey, A. K. 1990 *React. Solids* **8**, 211.

Galwey, A. K. 1992 *J. Thermal Anal.* **38**, 99.

Galwey, A. K. & Guarini, G. G. T. 1993 *Proc. R. Soc. Lond.* A **441**, 313.

Galwey, A. K., Koga, N. & Tanaka, H. 1990 *J. chem. Soc. Faraday Trans.* I **86**, 531.

Galwey, A. K. & Laverty, G. M. 1990*a* *J. Chim. Phys.* **87**, 1207.

Galwey, A. K. & Laverty, G. M. 1990*b* *Solid State Ionics* **38**, 155.

Galwey, A. K. & Laverty, G. M. 1993 *Proc. R. Soc. Lond* A **440**, 77.

Galwey, A. K., Laverty, G. M., Okhotnikov, V. B. & O'Neill, J. 1992 *J. Thermal Anal.* **38**, 421.

Galwey, A. K. & Mohamed, M. A. 1987 *Thermochim. Acta* **121**, 97.

Galwey, A. K. & Pöppl, L. 1984 *Phil. Trans. R. Soc. Lond.* A **311**, 159.

Galwey, A. K., Spinicci, R. & Guarini, G. G. T. 1981 *Proc. R. Soc. Lond.* A **378**, 477.

Downloaded from rsta.royalsocietypublishing.org

Garner, W. E. 1955 *Chemistry of the solid state*. London: Butterworth.

Guarini, G. G. T. & Piccini, S. 1988 *J. chem. Soc. Faraday Trans.* I **84**, 331.

Guarini, G. G. T. & Rustici, M. 1987 *React. Solids* **2**, 381.

Niepce, J.-C. & Watelle-Marion, G. 1973 *C.r. Acad. Sci., Paris* C **276**, 627.

Oswald, H. R. 1980 Thermal analysis. In *Proc. 6th Int. Conf.*, p. 1. Basel: Birkhäuser.

Sheen, D. B. & Sherwood, J. N. 1985 Reactivity of solids. In *Proc. 10th Int. Symp.*, p. 93. Amsterdam: Elsevier. (See also *Chem. Br.* **22**, 535 (1986).)

Received 4 November 1992; accepted 5 February 1993

PHILOSOPHICAL TRANSACTIONS OF THE ROYAL SOCIETY A MATHEMATICAL, PHYSICAL & ENGINEERING SCIENCES

PHILOSOPHICAL TRANSACTIONS OF THE ROYAL SOCIETY A MATHEMATICAL, PHYSICAL & ENGINEERING SCIENCES

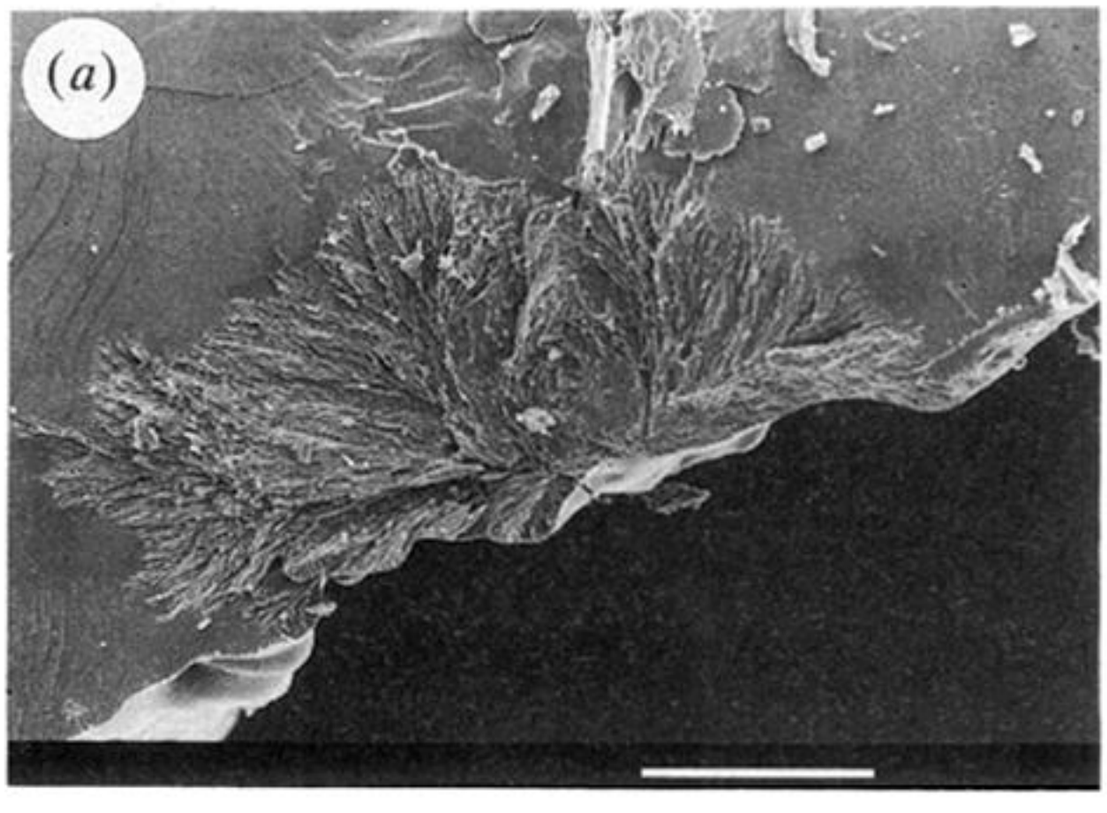

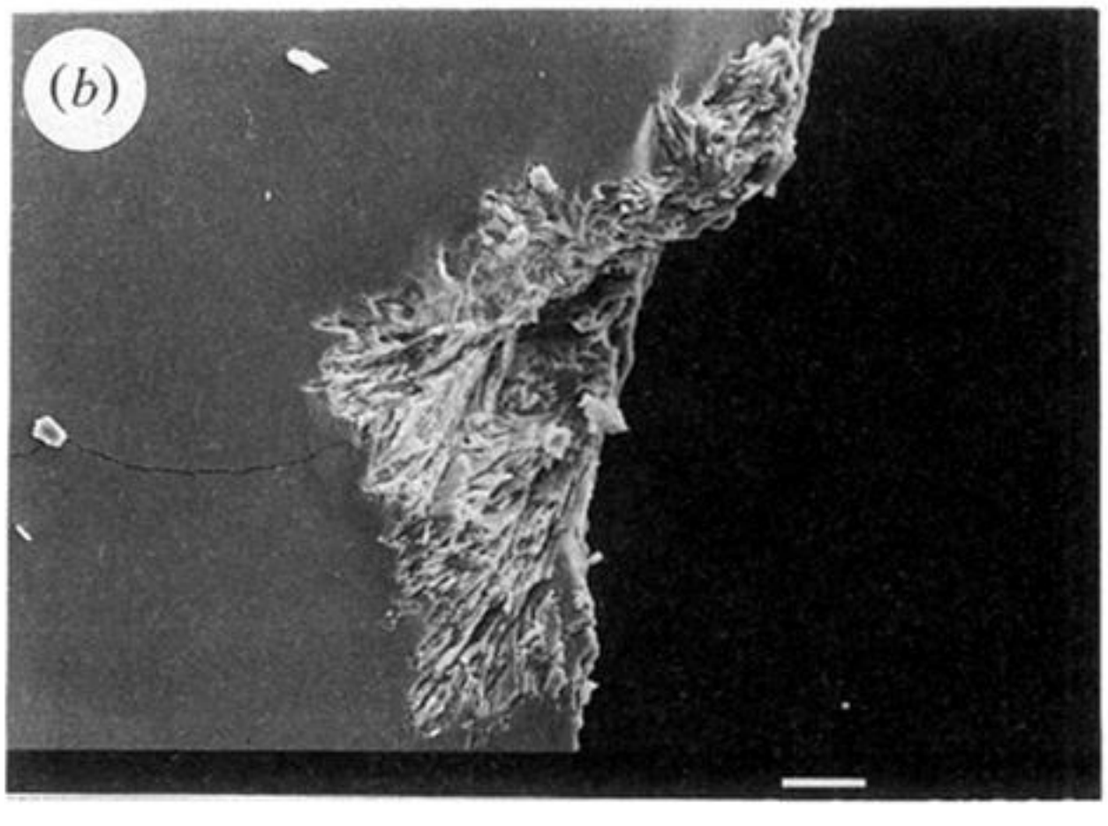

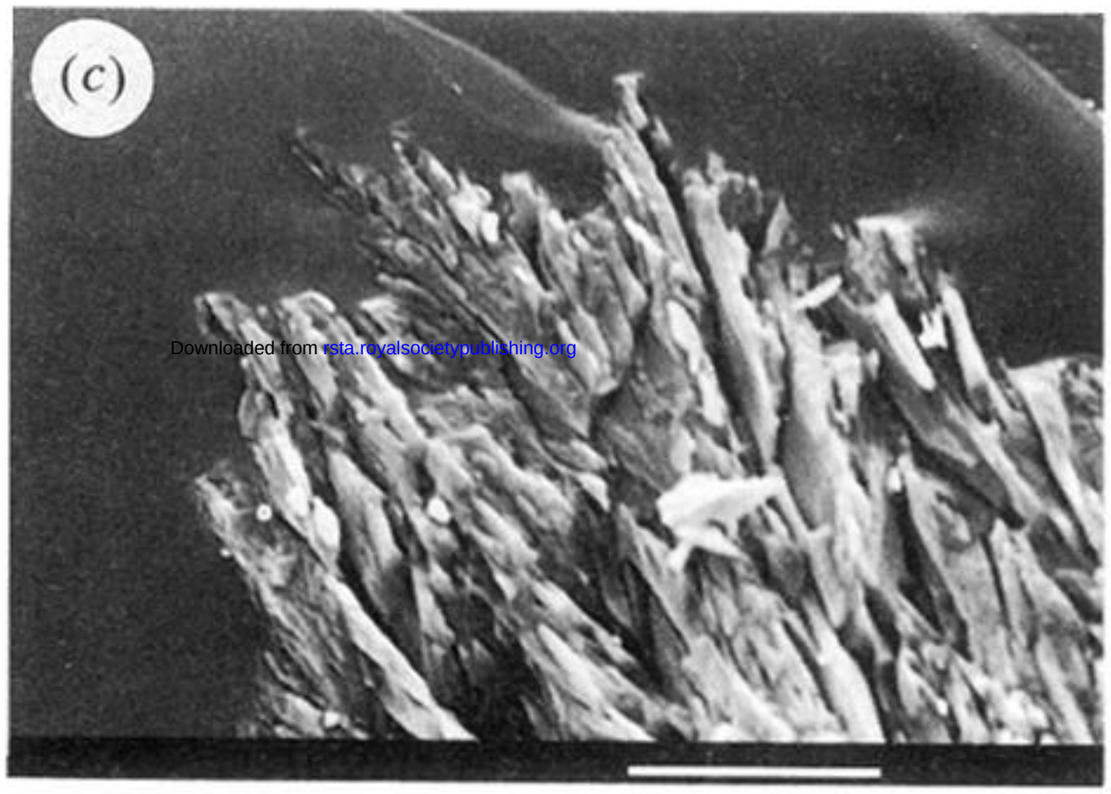

Downloaded from rsta.royalsocietypublishing.org

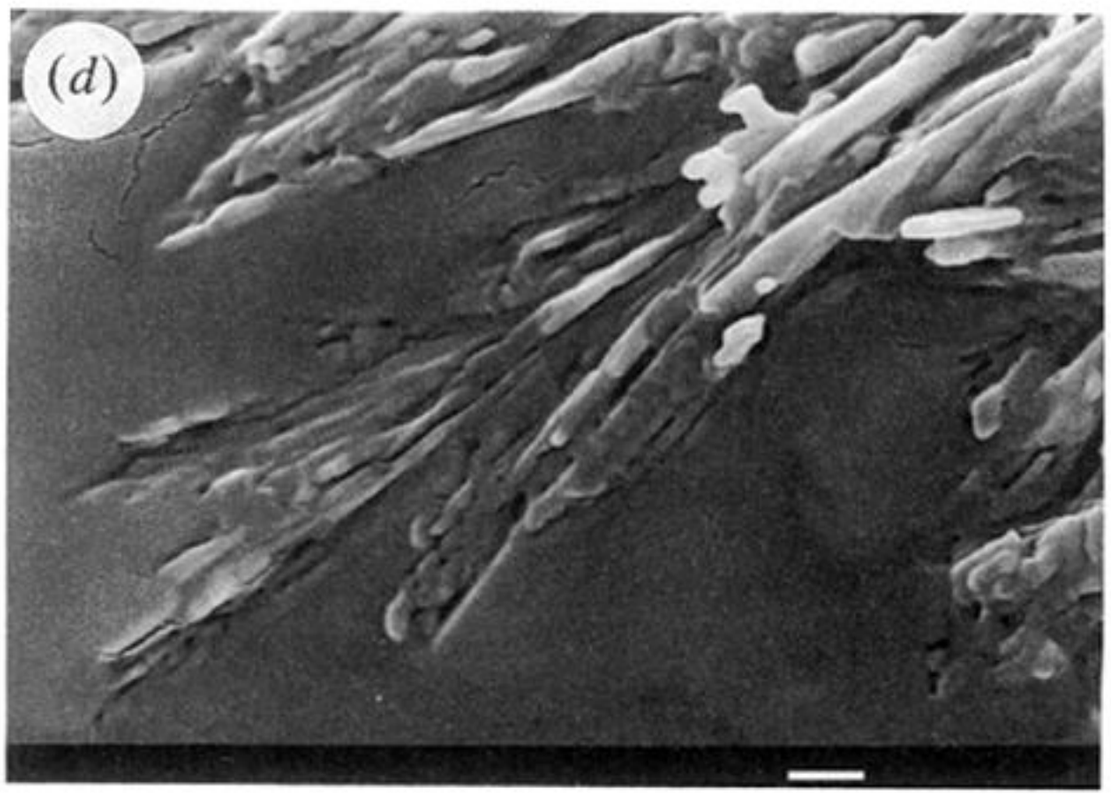

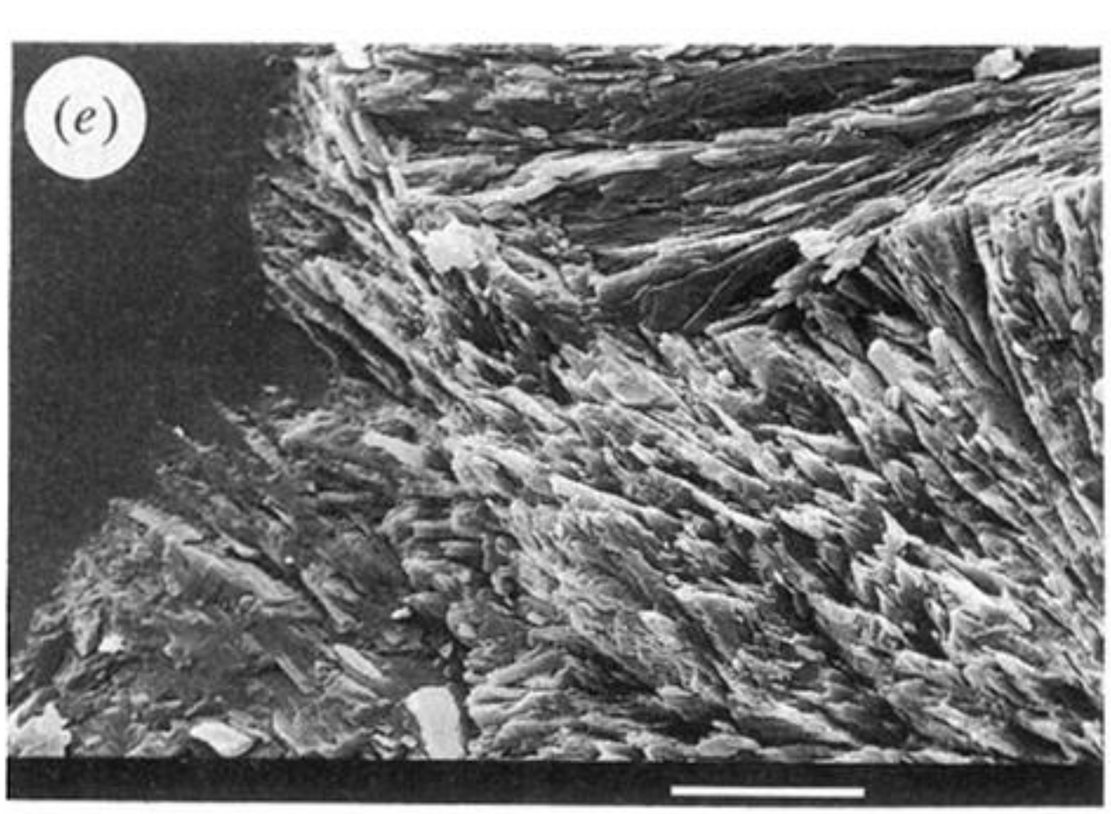

Figure 3. Partly dehydrated single crystal of *d*-$LiKC_4H_4O_6 . H_2O$ ($\alpha = 0.12$ at 434 K) cleaved after reaction to show textured nuclei in section together with the relatively smooth unreacted material. Intranuclear crystallites are of length *ca.* 10 μm, thickness *ca.* 1 μm, and show alignment. (Scale bars: (*a*) 100 μm; (*b*), (*c*), (*e*) 10 μm; (*d*) 1.0 μm.)

PHILOSOPHICAL TRANSACTIONS OF THE ROYAL SOCIETY A MATHEMATICAL, PHYSICAL & ENGINEERING SCIENCES

Figure 4

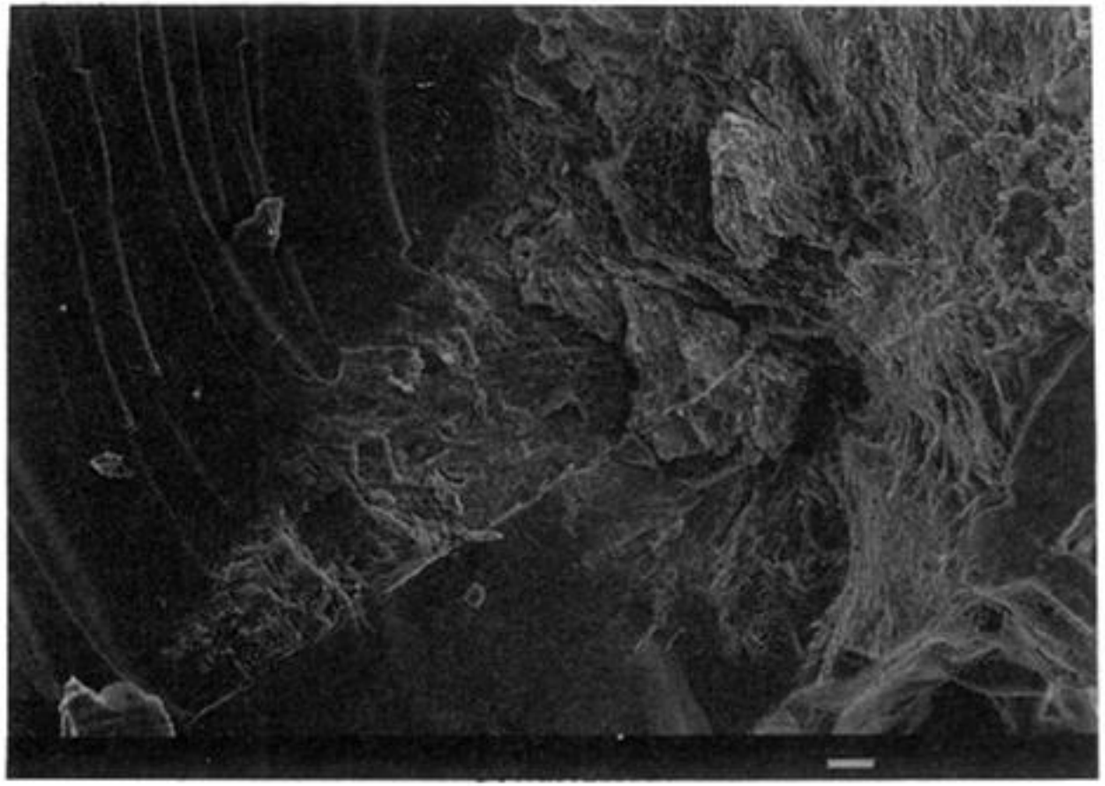

Figure 5

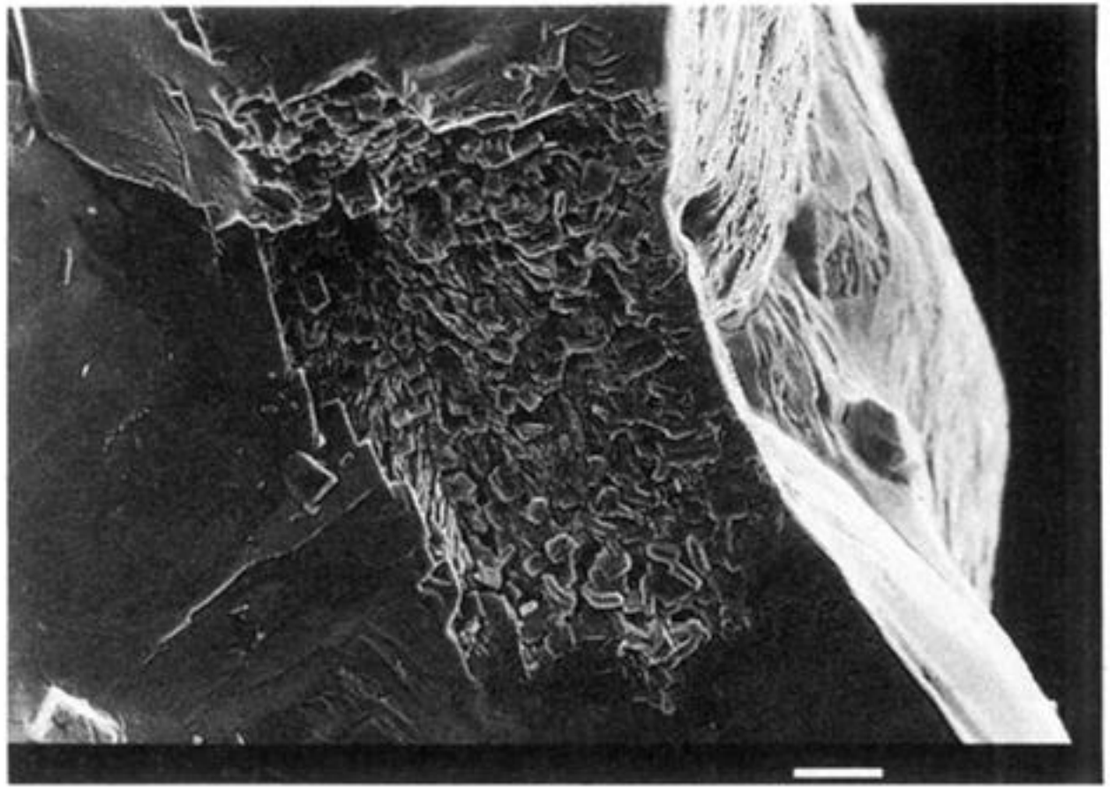

igure 4. Section of a partly dehydrated single crystal of *d*-$LiKC_4H_4O_6.H_2O$ ($\alpha = 0.20$ at 423 K), nowing extended nucleus growth along one side of a crack present before reaction. (Scale bar) μm.)

igure 5. Section of a partly dehydrated single crystal of *d*-$LiKC_4H_4O_6.H_2O$ ($\alpha = 0.14$ at 420 K). he nucleus is located beneath a texturally modified crystal face. (Scale bar 10 μm.)

Figure 6

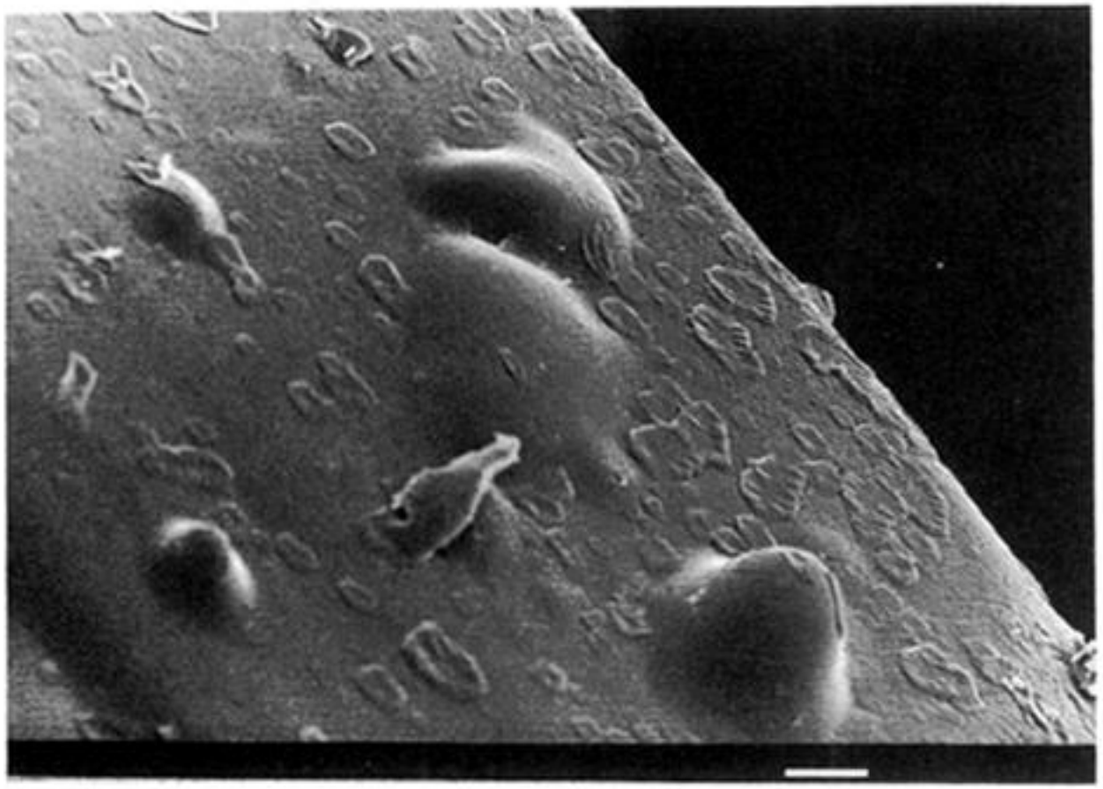

Figure 7

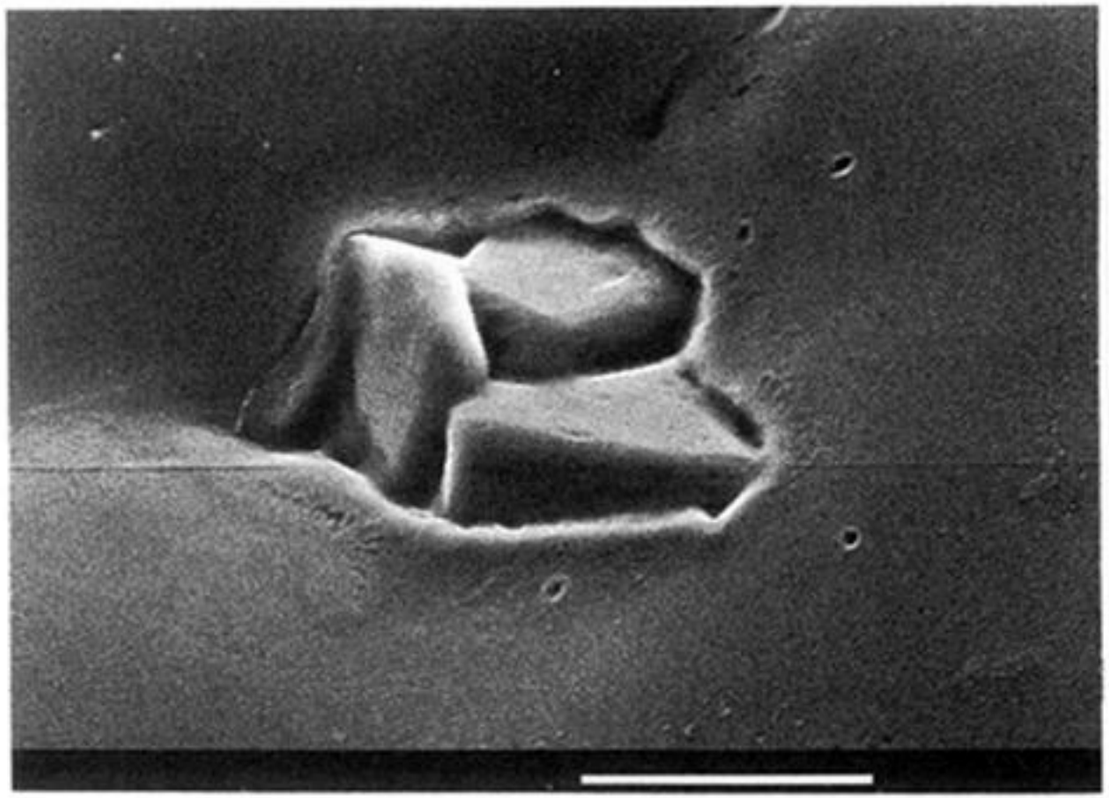

igure 6. Surface of a partly dehydrated single crystal of *d*-$LiKC_4H_4O_6.H_2O$ ($\alpha = 0.14$ at 420 K). lister-like modifications are identified as accumulations of water vapour before its release. (Scale ar 10 μm.)

igure 7. Surface of a partly dehydrated single crystal of *d*-$LiKC_4H_4O_6.H_2O$ ($\alpha = 0.42$ at 425 K). rare occurrence of surface penetration by crystalline material. (Scale bar 10 μm).

PHILOSOPHICAL TRANSACTIONS OF THE ROYAL SOCIETY A MATHEMATICAL, PHYSICAL & ENGINEERING SCIENCES

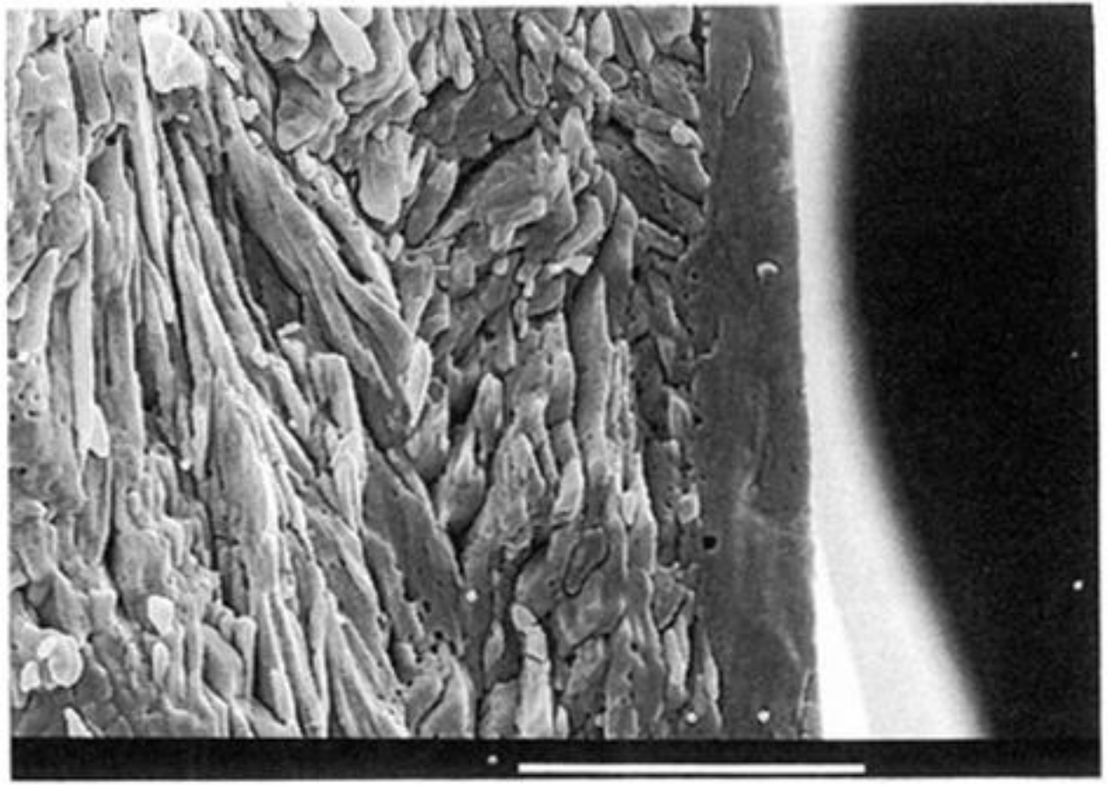

igure 8. Section of a reacted zone in a partly dehydrated single crystal of *d*-$LiKC_4H_4O_6.H_2O$ ($\alpha = 0.15$ at 433 K). The outer coherent layer identified with the first reaction has a different exture from the small intranuclear product crystallites generated beneath. (Scale bar 10 μm.)

PHILOSOPHICAL TRANSACTIONS OF THE ROYAL SOCIETY A MATHEMATICAL, PHYSICAL & ENGINEERING SCIENCES

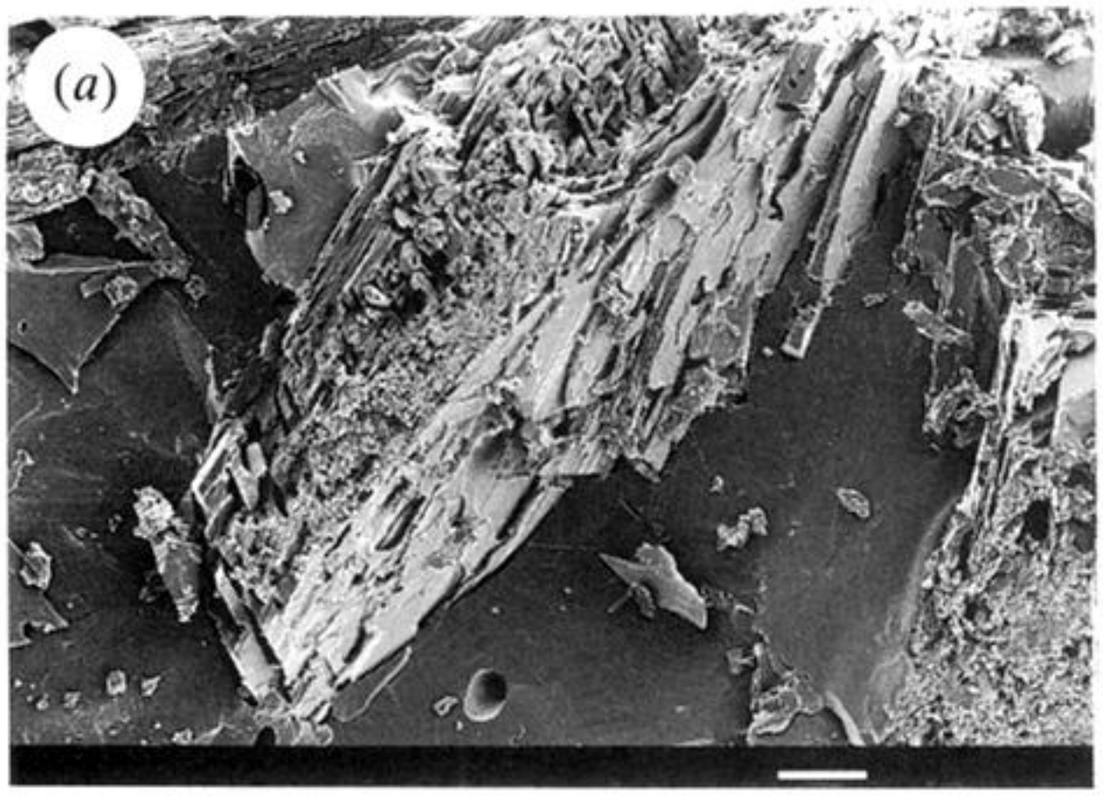

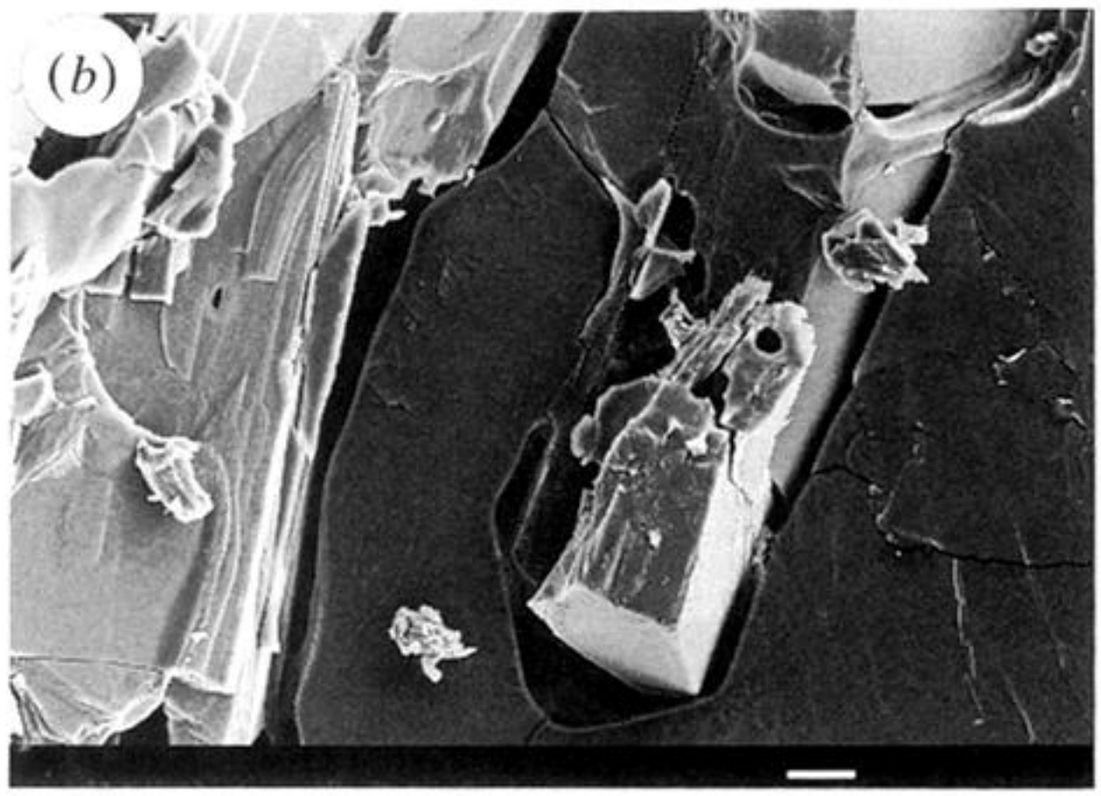

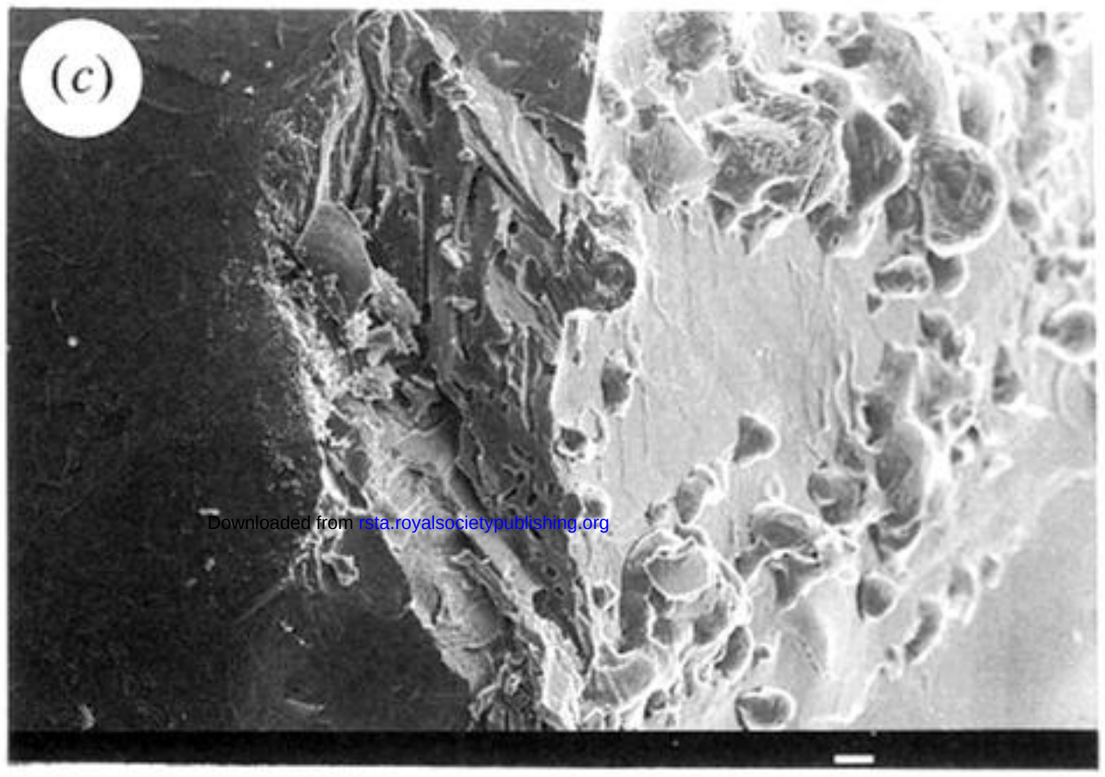

Downloaded from rsta.royalsocietypublishing.org

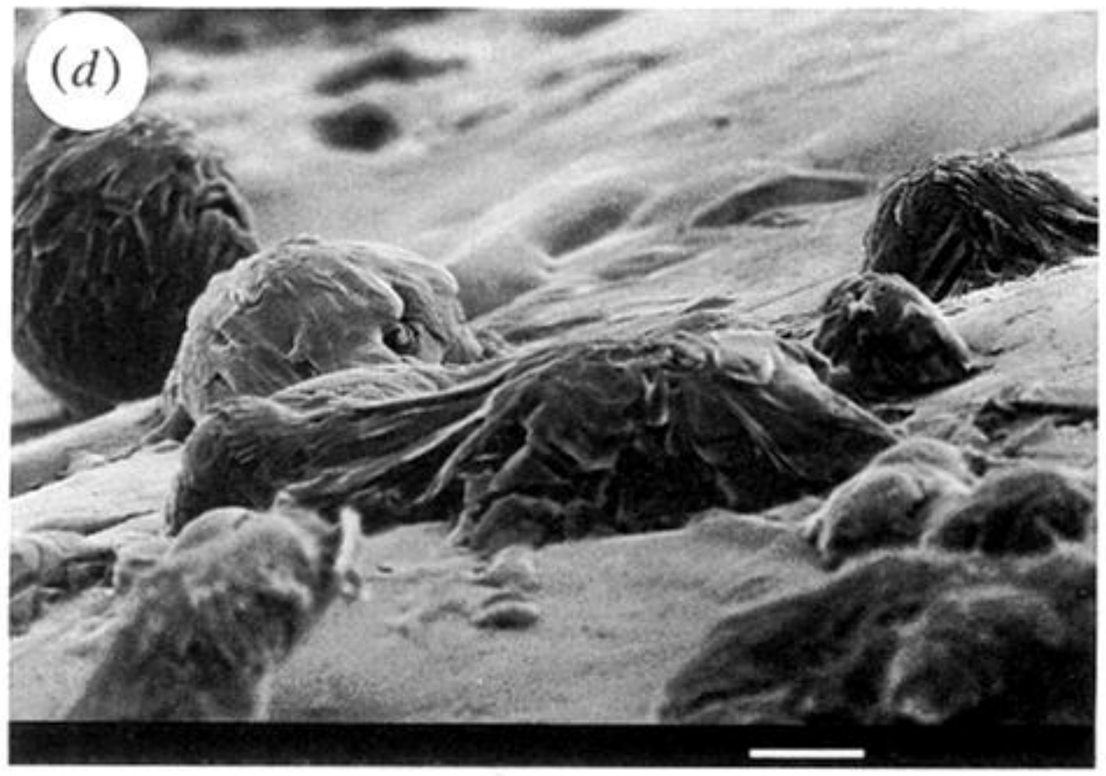

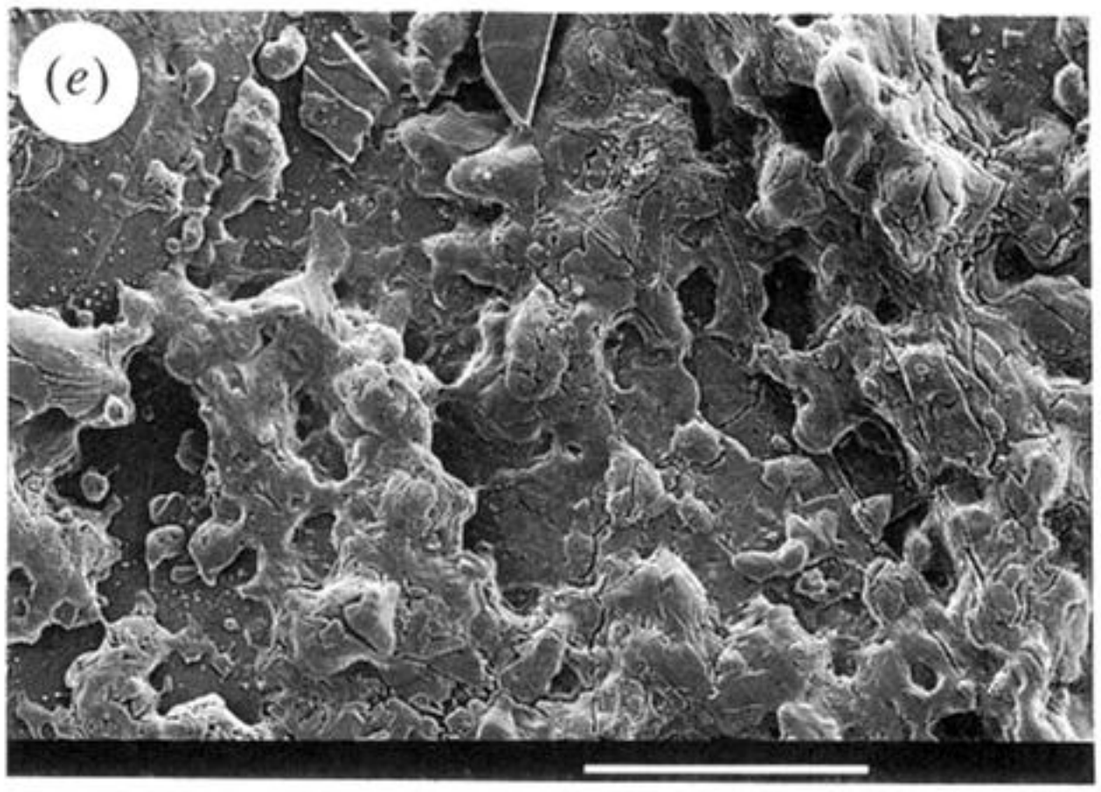

Figure 9. Sections (*a*), (*b*), (*c*) and surfaces (*d*), (*e*) of a partly dehydrated single crystal of *d*-$NaKC_4H_4O_6 . H_2O$ ($\alpha = 0.40$ at 460 K). At this higher reaction temperature contact between product and reactant at nucleus peripheries is reduced by the generation of channels. Outer surfaces are distorted and show evidence of local liquefaction together with bubbles that are associated with release of product water vapour from nuclei beneath. (Scale bars: (*a*), (*e*) 100 μm; (*b*), (*c*), (*d*) 50 μm.)

PHILOSOPHICAL TRANSACTIONS OF THE ROYAL SOCIETY A MATHEMATICAL, PHYSICAL & ENGINEERING SCIENCES

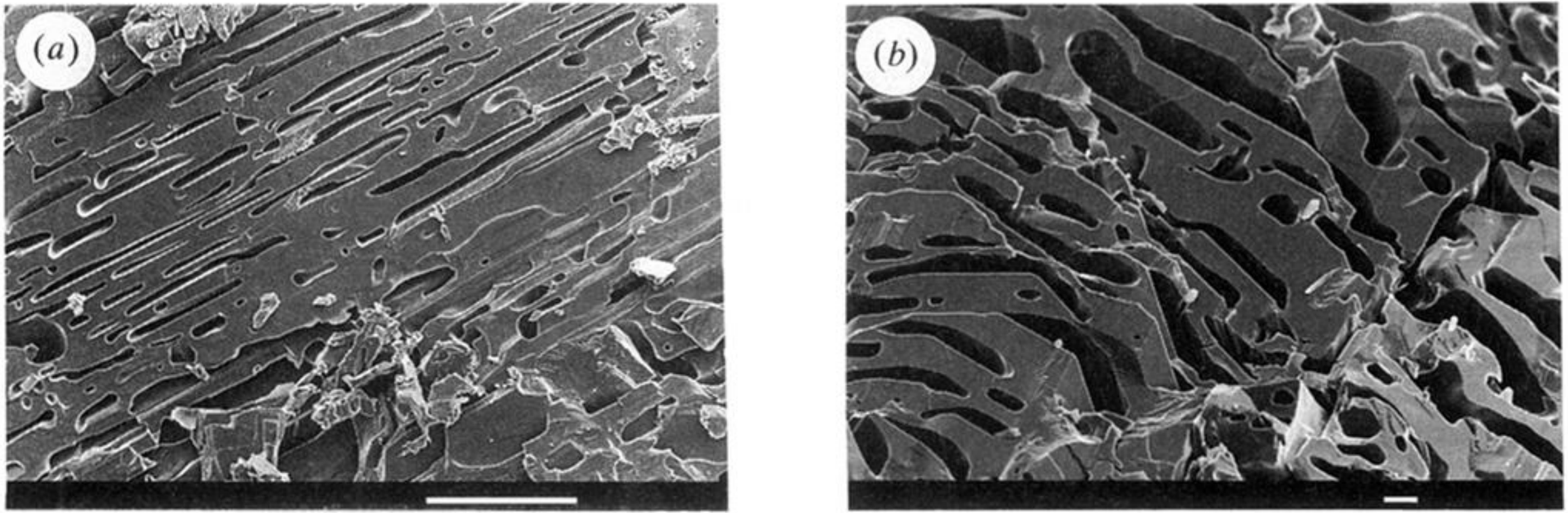

Figure 10. Cleaved single crystal of *d*-$LiKC_4H_4O_6.H_2O$, after complete dehydration ($\alpha = 1.00$ at 463 K). Pores in the product are rounded, elongated and show some parallelism. (Scale bars: (*a*) 100 μm; (*b*) 10 μm.)

PHILOSOPHICAL TRANSACTIONS OF THE ROYAL SOCIETY A MATHEMATICAL, PHYSICAL & ENGINEERING SCIENCES

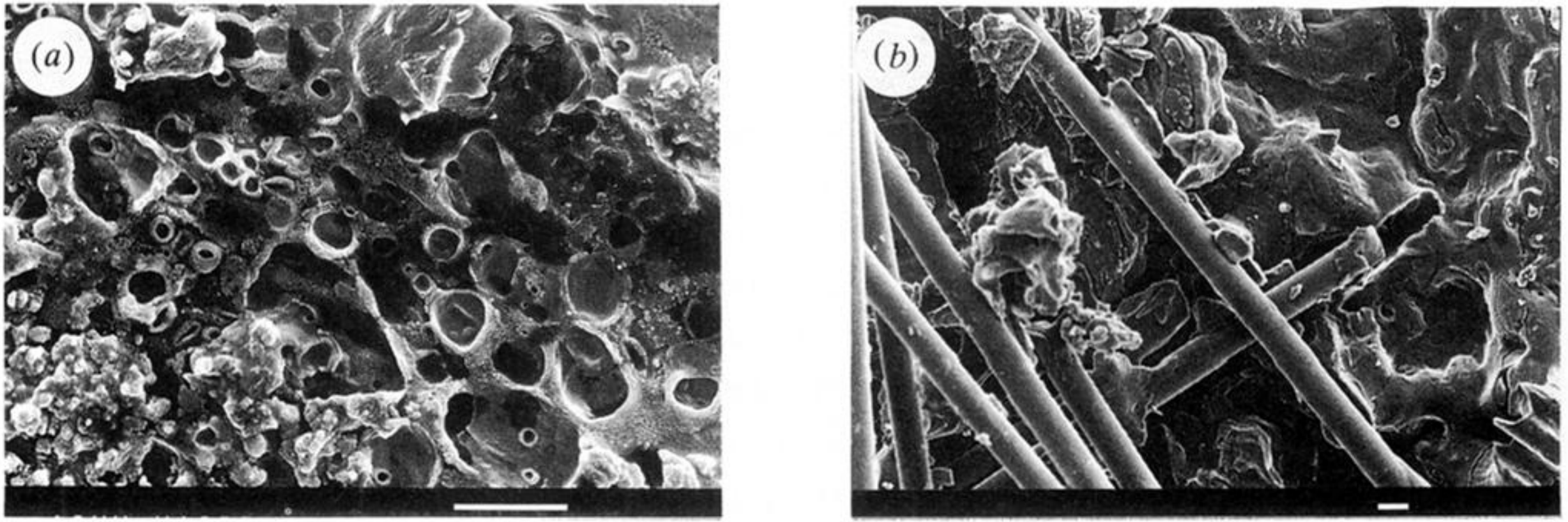

igure 11. Surfaces of a single crystal of *d*-$LiKC_4H_4O_6 . H_2O$ after complete dehydration ($\alpha = 1.00$ t 455 K). Crystal features are absent, and the burst bubbles and penetration by glass fibres are vidence of superficial liquefaction. (Scale bars both 10 μm.)

PHILOSOPHICAL TRANSACTIONS OF THE ROYAL SOCIETY A MATHEMATICAL, PHYSICAL & ENGINEERING SCIENCES

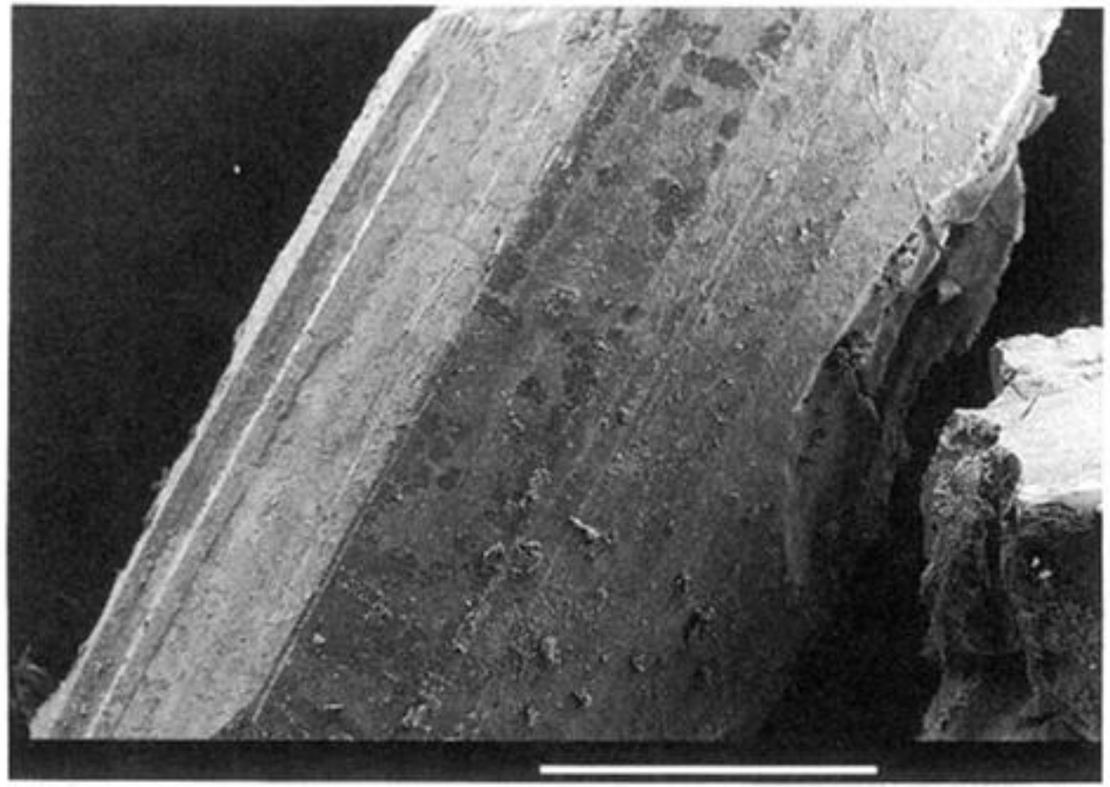

igure 12. Crystal of *d*-$LiKC_4H_4O_6.H_2O$ after complete dehydration ($\alpha = 1.00$ at 425 K) initially rrounded loosely by crushed, dehydrated product. The anhydrous powder did not significantly dhere to the reactant crystal. (Scale bar 1 mm.)

PHILOSOPHICAL TRANSACTIONS OF THE ROYAL SOCIETY A MATHEMATICAL, PHYSICAL & ENGINEERING SCIENCES

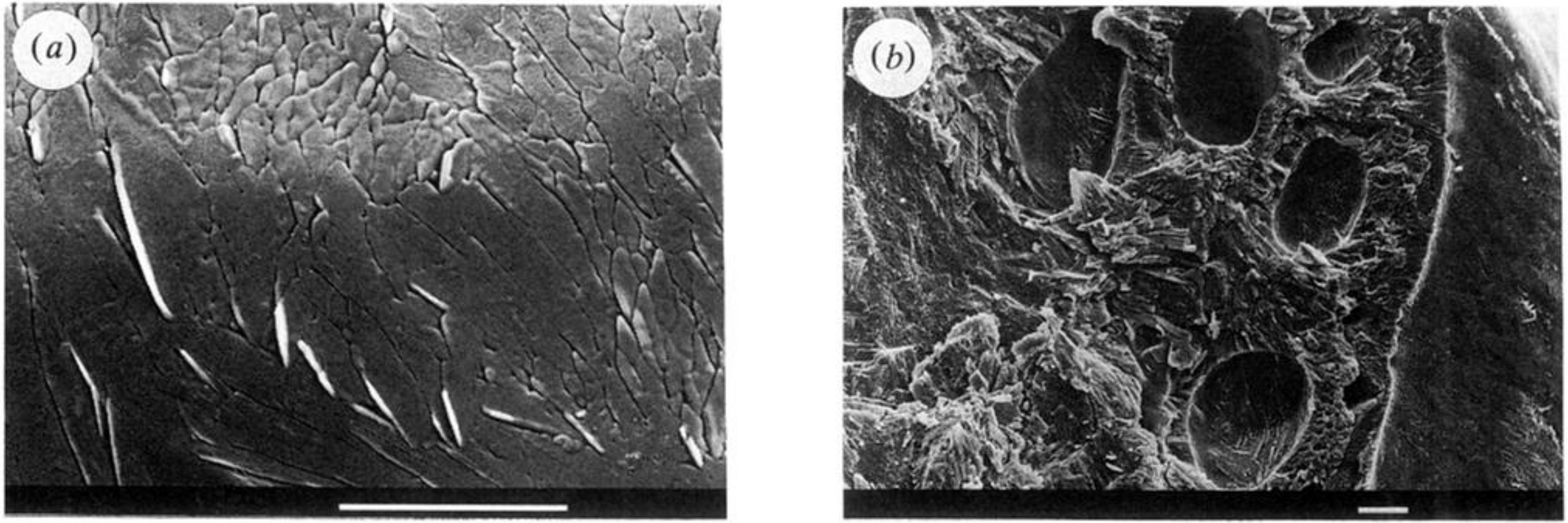

Figure 13. Surface (*a*) and section (*b*) of a crystal of *d*-$LiKC_4H_4O_6 . H_2O$, dehydrated ($\alpha = 1.00$) at 323 K, in the presence of water vapour admitted before reaction. External crystal faces are smoother and large pores develop in the crystal bulk. (Scale bars both 10 μm.)

PHILOSOPHICAL TRANSACTIONS OF THE ROYAL SOCIETY A MATHEMATICAL, PHYSICAL & ENGINEERING SCIENCES

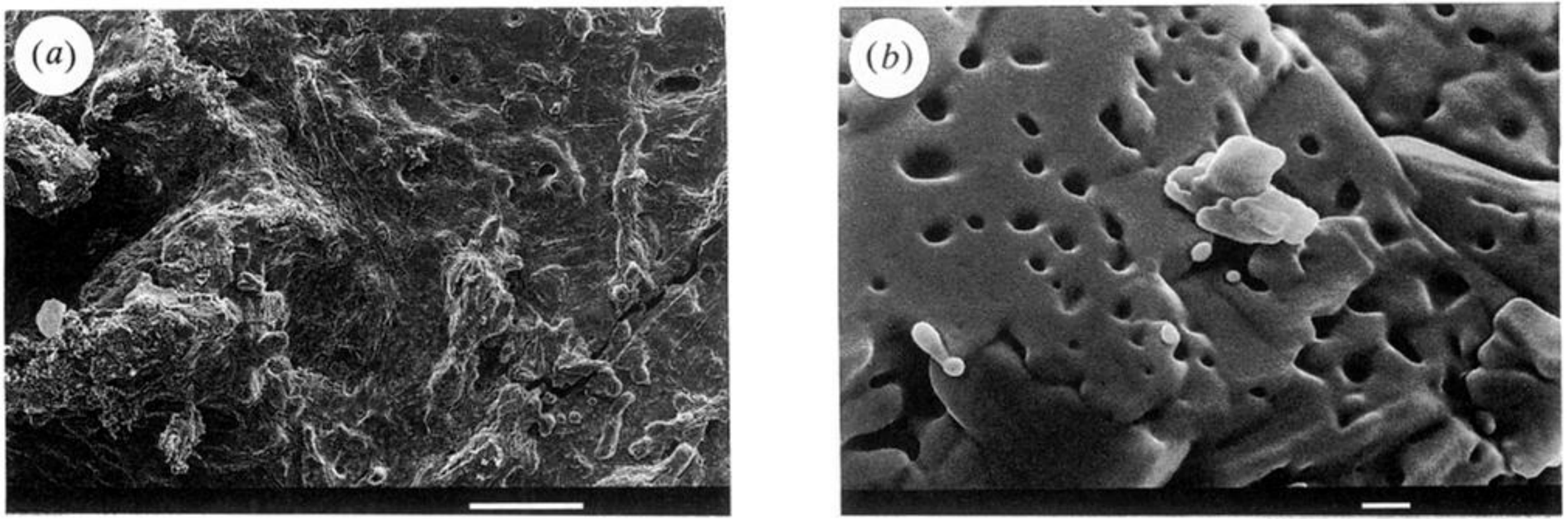

igure 14. Surface of a crystal of *d*-$LiKC_4H_4O_6.H_2O$ after two successive dehydrations ($\alpha = 1.00$; 461 K and 423 K) with intermediate rehydration at 290 K. Features are smooth and rounded, ndicating a superficial boundary layer controlled by surface tension forces. (Scale bars (*a*) 100 μm;) 1.0 μm.)

PHILOSOPHICAL TRANSACTIONS OF THE ROYAL SOCIETY A MATHEMATICAL, PHYSICAL & ENGINEERING SCIENCES
PHILOSOPHICAL TRANSACTIONS OF THE SOCI

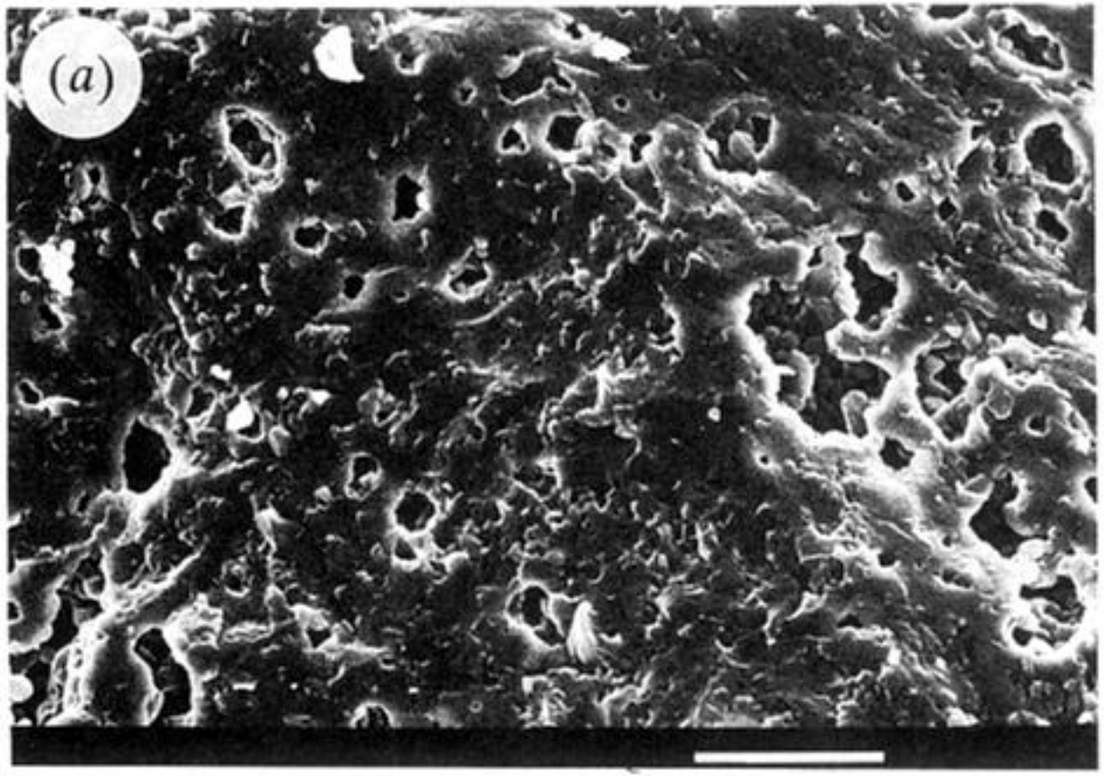

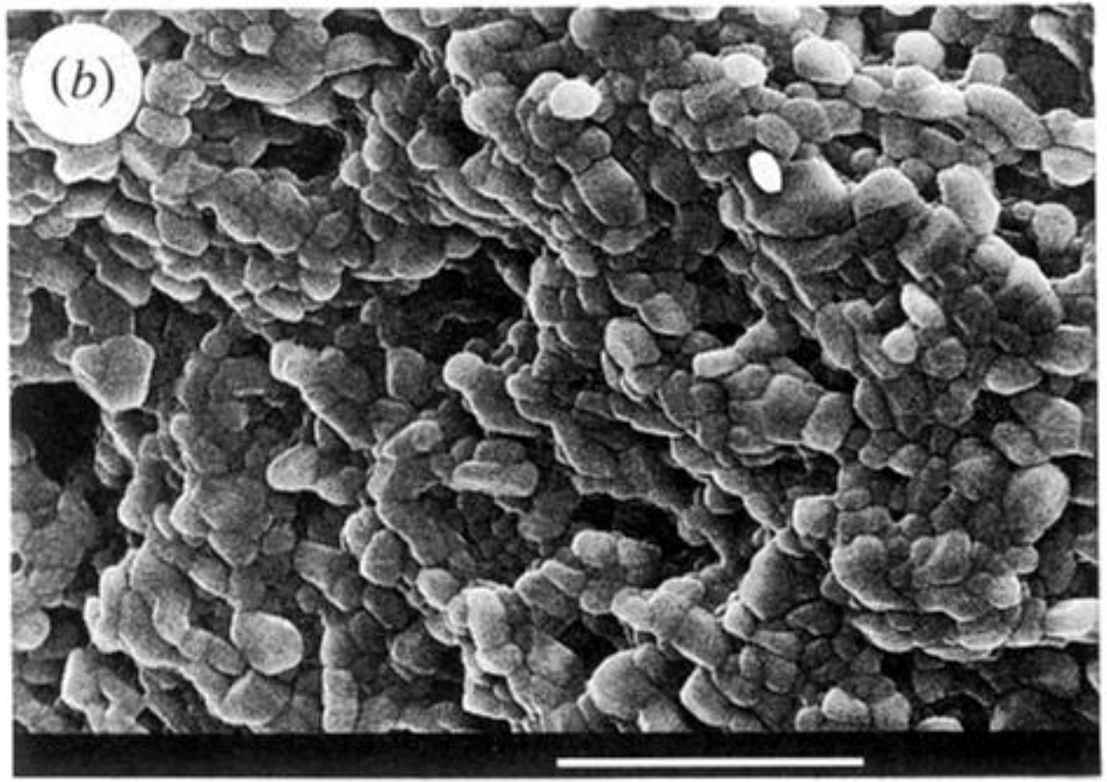

igure 15. Surface and internal textures of a crystal ($\alpha = 1.00$) of d-$LiKC_4H_4O_6.H_2O$ after seven uccessive dehydration/rehydration cycles (at 423 K and 290 K respectively). The surface (a) is pproximately planar but porous, while the internal texture (b) is composed of small crystallites. Scale bars both 10 μm.)

PHILOSOPHICAL TRANSACTIONS OF THE ROYAL SOCIETY A MATHEMATICAL, PHYSICAL & ENGINEERING SCIENCES

Downloaded from rsta.royalsocietypublishing.org

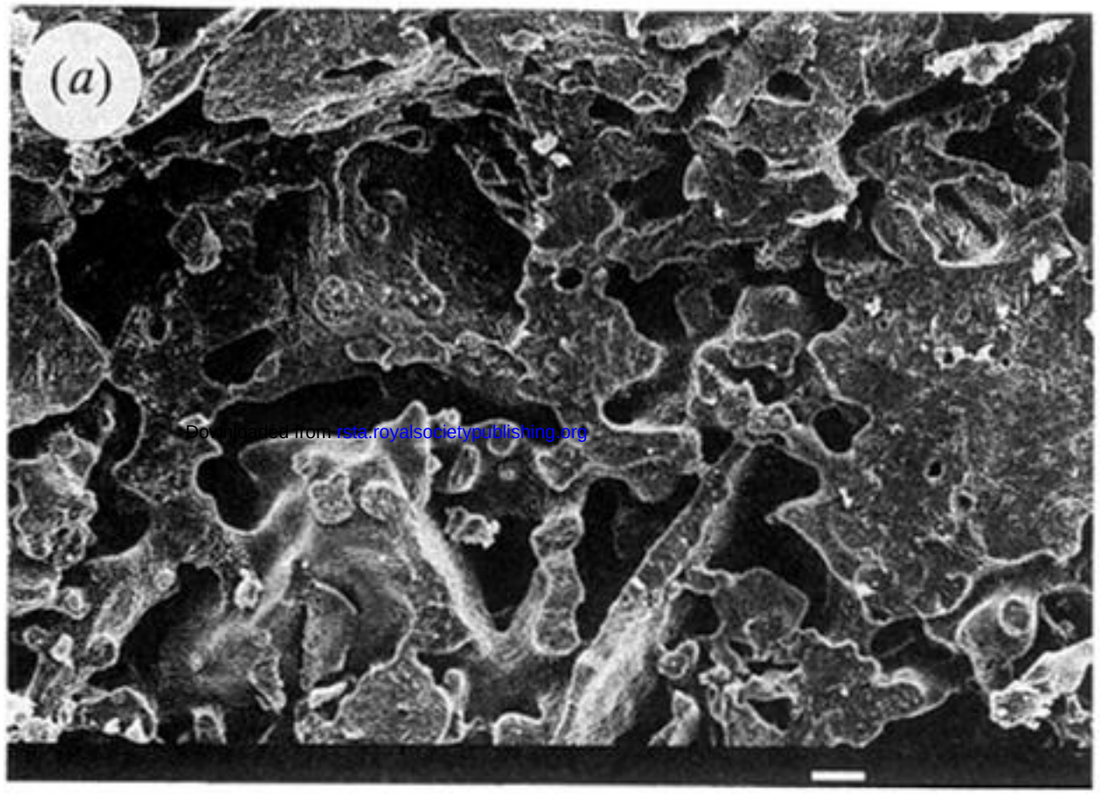

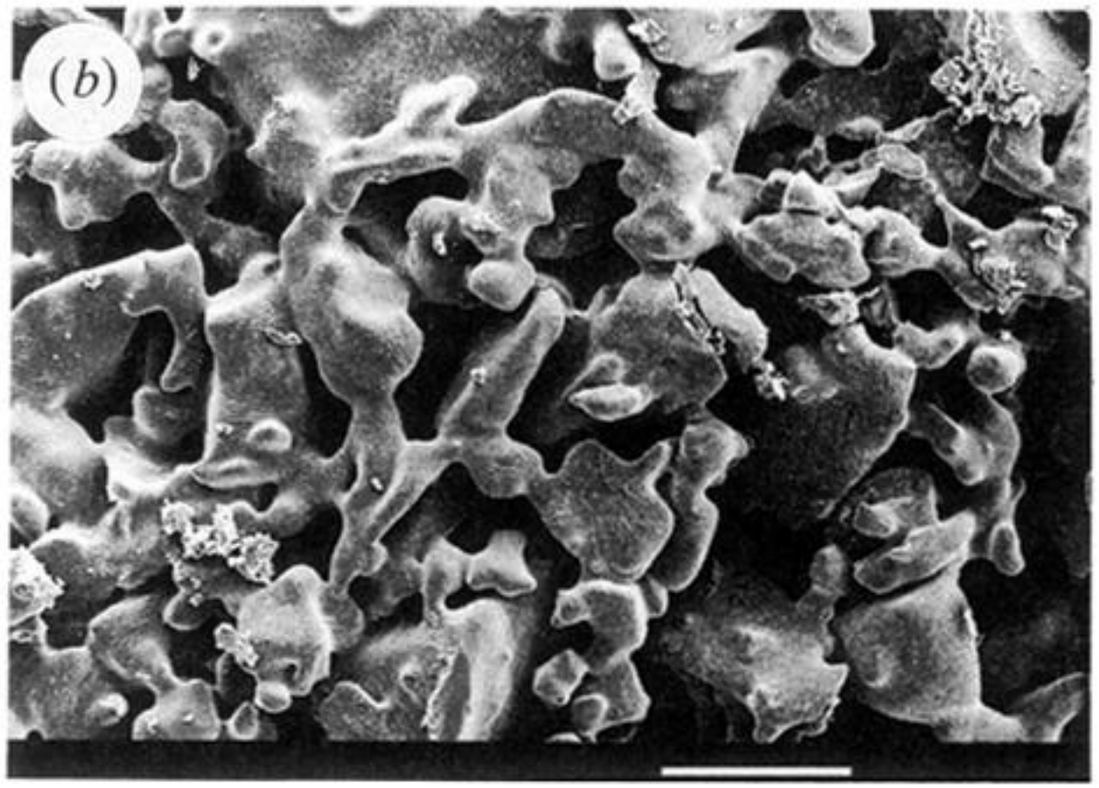

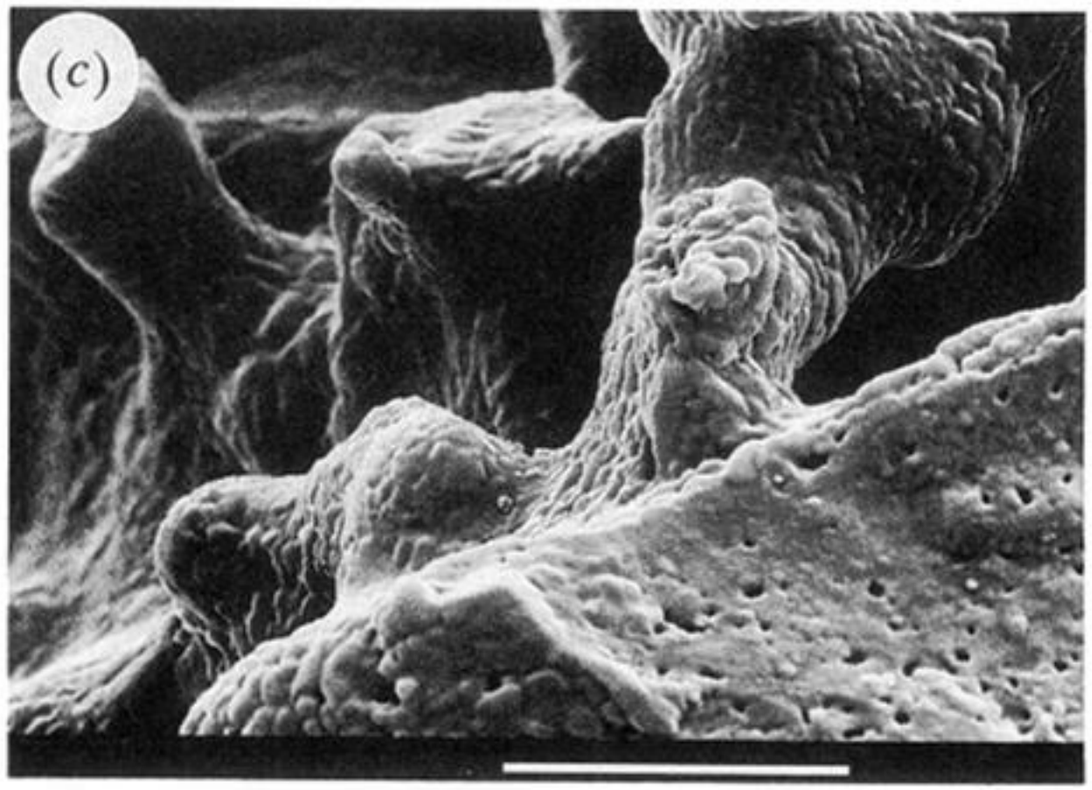

Figure 16. (*a*), (*c*) Crushed *d*-$LiKC_4H_4O_6.H_2O$ after dehydration ($\alpha = 1.0$ at 423 K) commencing in vacuum. Sintering particles make contact by fusion of the vitreous or semi-molten surface layer. (Scale bars both 10 μm.) (*b*) Crushed *d*-$LiKC_4H_4O_6.H_2O$ after dehydration at 423 K started with 1050 Pa of initial water vapour. (Scale bar 100 μm.)

PHILOSOPHICAL TRANSACTIONS OF THE ROYAL SOCIETY A MATHEMATICAL, PHYSICAL & ENGINEERING SCIENCES

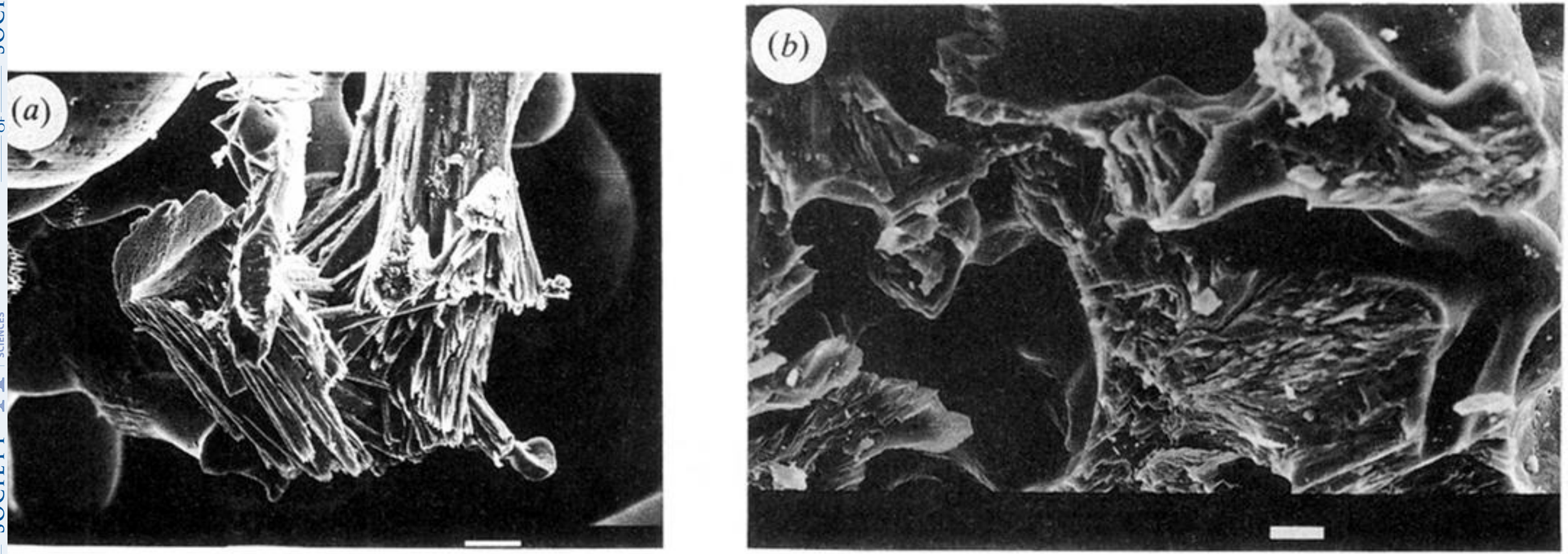

Figure 17. Centre of d-$LiKC_4H_4O_6 . H_2O$ crystallites after dehydration ($\alpha = 1.0$ at 423 K). Textures of the product particles composing the nuclei are similar to those found in single crystals (figures 3–4). (Scale bars both 10 μm.)

PHILOSOPHICAL TRANSACTIONS OF THE ROYAL SOCIETY A MATHEMATICAL, PHYSICAL & ENGINEERING SCIENCES

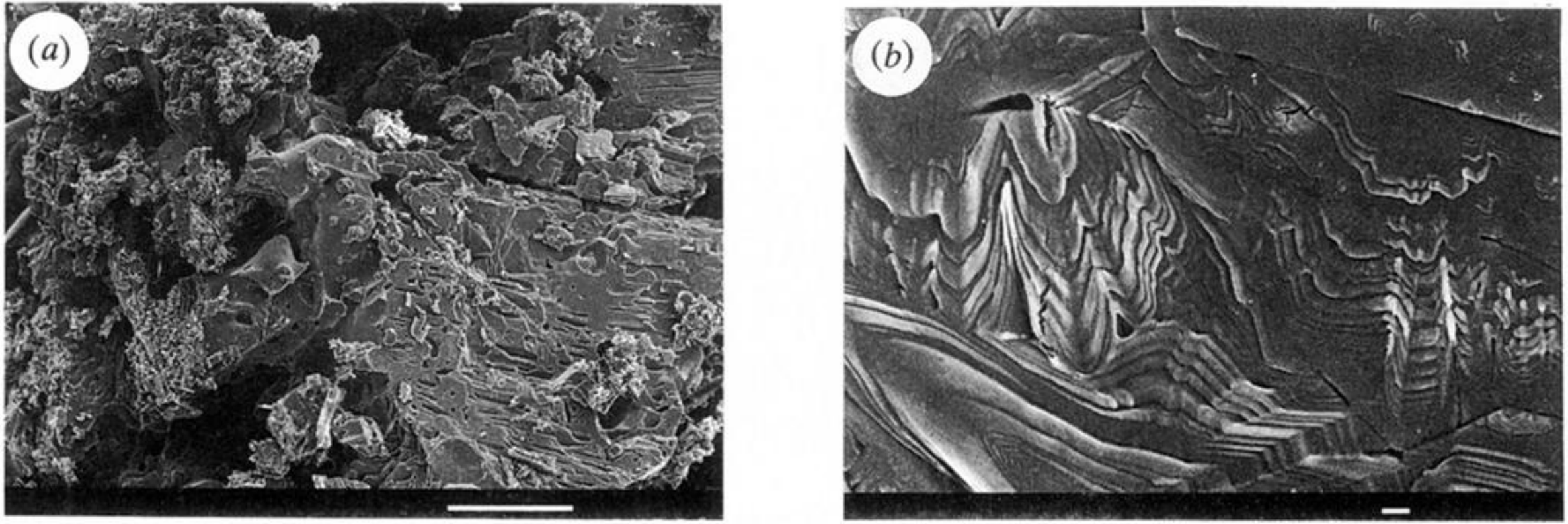

Figure 18. Powdered *d*-$LiKC_4H_4O_6.H_2O$ after dehydration ($\alpha = 1.00$ at 463 K). Textures of product salt are similar to those found in single crystals dehydrated at relatively higher temperatures (figure 10*a*, *b*). There is evidence of extensive sintering of the recrystallized outer surface. (Scale bar: (*a*) 100 μm; (*b*) 1.0 μm.)

PHILOSOPHICAL TRANSACTIONS OF THE ROYAL SOCIETY A MATHEMATICAL, PHYSICAL & ENGINEERING SCIENCES